Methane-oxidizing seawater microbial communities from an Arctic shelf

Christiane Uhlig[1]*, John B. Kirkpatrick[1,2], Steven D'Hondt[1], Brice Loose[1]

[1] Graduate School of Oceanography, University of Rhode Island, Narragansett, RI 02882, USA

[2] The Evergreen State College, Olympia, WA, 98505, USA

*current address: Alfred Wegener Institute Helmholtz Centre for Polar and Marine Research, Bremerhaven, 27570, Germany

Correspondence to: Christiane Uhlig (cuhlig@uri.edu)

Abstract. Marine microbial communities can consume dissolved methane before it has a chance to escape to the atmosphere and contribute to greenhouse warming. Seawater over the shallow Arctic shelf is characterized by excess methane compared to atmospheric equilibrium. This methane originates in sediment, permafrost and hydrate. Particularly high concentrations are found beneath sea ice. We studied the structure and methane oxidation potential of the microbial communities from seawater collected close to Utqiagvik, Alaska, in April 2016. The in situ methane concentrations were 16.3 ± 7.2 nmol L^{-1}, approximately 4.8 times oversaturated relative to atmospheric equilibrium. The group of methane-oxidizing bacteria (MOB) in the natural seawater and incubated seawater was >97% dominated by Methylococcales (γ-Proteobacteria). Incubations of seawater under a range of methane concentrations led to loss of diversity in the bacterial community. The abundance of MOB was low with maximal fractions of 2.5% at 200 times elevated methane concentration, while sequence reads of non-MOB methylotrophs were four times more abundant than MOB in most incubations. The abundances of MOB as well as non-MOB methylotroph sequences correlated tightly with the rate constant (k_{ox}) for methane oxidation, indicating that non-MOB methylotrophs might be coupled to MOB and involved in community methane oxidation. In sea ice, where methane concentrations of 82 ± 35.8 nmol kg^{-1} were found, *Methylobacterium* (α-Proteobacteria) was the dominant MOB with a relative abundance of 80%. Total MOB abundances were very low in sea ice, with maximal fractions found at the ice-snow interface (0.1%), while non-MOB-methylotrophs were present in abundances similar to natural seawater communities. The dissimilarities in MOB taxa, methane concentrations and stable isotope ratios between sea ice and water column point toward different methane cycling processes in the two environments.

1 Introduction

Methane (CH_4) is the third most abundant greenhouse gas contributing to climate change (IPCC, 2014) – exceeded only by water vapor and carbon dioxide. Despite much lower concentrations than carbon dioxide, it has a 28x higher accumulative radiative forcing potential (IPCC, 2014) over a time span of 100 years. In the ocean, the two major sources of methane are ongoing biogenic production by microbes in anoxic sediment (Formolo, 2010; Reeburgh, 2007; Whiticar, 1999) and release of fossil methane from geological storage (summarized by Kvenvolden and Rogers, 2005; Saunois et al., 2016). Other

sources include release from permafrost, river runoff, submarine groundwater discharge (Lecher et al., 2016; Overduin et al., 2012) and production from methylated substrates under aerobic conditions (Damm et al., 2010; Karl et al., 2008; Repeta et al., 2016). More than 90% of the methane sourced in the seabed is oxidized within the sediment by anaerobic and aerobic oxidation (Barnes and Goldberg, 1976; Boetius and Wenzhöfer, 2013; Knittel and Boetius, 2009; Reeburgh, 1976). The

5 remaining methane either diffuses into the water at the sediment surface, or is released as bubbles, which completely or partially dissolve while rising through the water column (Leifer and Patro, 2002). Dissolved methane is used as a substrate and oxidized by aerobic methanotrophic bacteria (methane-oxidizing bacteria, MOB) in the water column (Hanson and Hanson, 1996; Murrell, 2010) or diluted by the surrounding water column (e.g. Gentz et al., 2014). As a result of these biological and physical processes, oceanic methane concentrations are frequently at low nanomolar levels, leaving only a

10 small fraction of subseafloor-sourced methane to eventually exchange with the atmosphere (Karl et al., 2008; Reeburgh, 2007).

By contrast, in the Subarctic and Arctic shelf areas, shallow water depths and seasonal sea ice cover complicate the picture. High concentrations of methane have been reported from the entire water column up to the surface around Svalbard (Damm et al., 2005; Mau et al., 2013), the Siberian Shelf (Shakhova et al., 2010) and the Beaufort Sea (Lorenson et al., 2016). In

15 addition, during periods of near 100% sea ice cover, gas exchange from the water column to the atmosphere is restricted (Loose et al., 2011). While under ice free conditions, methane concentrations are frequently found in the range of 15 to 30 nmol L^{-1} or around 700% supersaturated with regard to atmospheric equilibrium, winter concentrations are often 10 to 100 times higher. Maximal concentrations of 5000 nmol L^{-1}, oversaturation of 160000%, have been reported from the Siberian Shelf (Lorenson et al., 2016; Shakhova et al., 2010; Zhou et al., 2014).

20 Along with factors like oxygen and trace metal availability (Crespo-Medina et al., 2014; Sansone et al., 2001; Semrau et al., 2010), dissolved methane concentration is an important control on the community of MOB and thus methane oxidation rates (Crespo-Medina et al., 2014; Kessler et al., 2011; Mau et al., 2013). Methane hotspots, promoted by limited gas exchange under sea ice, might thus be candidate regions for accumulation of methane oxidizers. In addition, sea ice, particular the ice-water interface, is a hotspot for microbial activity. The ice surface, penetration of light, and constant exchange with the

25 underlying water column favor the development of communities composed of small eukaryotic organisms, microalgae, prokaryotes and viruses; the biomass often being several orders of magnitudes denser than in the underlying water column (Thomas and Dieckmann, 2002).

Methane-oxidizing bacteria use methane as their sole carbon and energy source (Hanson and Hanson, 1996). In the first step, methane is oxidized to methanol catalyzed by the enzyme methane monooxygenase. Since methane monooxygenase is

30 characteristic of nearly all MOB (Knief, 2015), *pmoA*, the gene encoding for a subunit of the membrane-bound particulate methanemono-oxygenase, has been used as a specific molecular marker for detection and characterization of MOB (Knief, 2015; Lüke and Frenzel, 2011; reviewed by McDonald et al., 2008; Tavormina et al., 2008). Methanol is further metabolized to formaldehyde, from which it is either mineralized to carbon dioxide (CO_2), or assimilated into organic compounds and finally biomass (reviewed by Hanson and Hanson, 1996; reviewed by Strong et al., 2015). Different types of MOB are

distinguished by their phylogeny and assimilation pathways for formaldehyde. While γ-Proteobacteria or Type I MOB assimilate formaldehyde via the ribulose monophosphate pathway (RuMP), α-Proteobacteria or Type II MOB use the serine pathway (Hanson and Hanson, 1996). Besides these two proteobacterial groups, MOB also occur in the phylum Verrucomicrobia (e.g. Dunfield et al., 2007; Pol et al., 2007).

5 Methane-derived carbon is also assimilated in non-methane utilizing methylotrophs (non-MOB methylotrophs) or other bacteria in freshwater and temperate marine environments. These non-methane oxidizers are suggested to cross-feed on metabolites produced by the MOB (Hutchens et al., 2003; Jensen et al., 2008; Saidi-Mehrabad et al., 2013).

Knowledge of the microbial communities responsible for methane oxidation in the Arctic and Subarctic is still sparse. During the last years, the first few studies have determined methane oxidation rates from seawater in these regions to cover a 10 range from 10^{-4} up to 3.2 nmol L^{-1} d^{-1} (Gentz et al., 2014; Lorenson et al., 2016; Mau et al., 2013, 2017; Steinle et al., 2015). In only two of these studies, both performed off Svalbard, oxidation rate measurements were combined with analysis of the microbial community. Steinle et al. (2015) quantified MOB by fluorescence in situ hybridization and microscopy. Low but relatively constant cell-specific oxidation rates were determined from the oxidation rates and MOB abundance, indicating that MOB community size is an important control on the total methane oxidation rate in the system. Mau et al. (2013) 15 analyzed the bacterial community with denaturing gradient gel electrophoresis (DGGE) of the 16S gene and compared patterns of PCR products for *pmoA*. Different MOB communities were observed in the meltwater layer and deep water in this stratified system, also reflecting the observed differences in methane oxidation rates. Only one of the eleven analyzed DGGE bands was identified as methanotroph (from the genus *Methylosphaera*) from the deep water in this study, while none were detected in the meltwater, possibly due to the limitations of the method. To our knowledge, no high-throughput 20 sequencing studies of methane-oxidizing bacteria in the Arctic have been published in peer-reviewed literature to date.

We studied methane-oxidizing communities from seawater sampled on the Beaufort Sea shelf close to Utqiagvik, Alaska. Incubation experiments were performed under different methane concentrations to directly compare the bacterial community structure with methane oxidation rates. Seawater incubations, freshly sampled sea water, and sea ice were analyzed for their entire community diversity (16S rDNA) and the presence of MOB (16S rDNA and *pmoA*) using high-throughput Illumina 25 MiSeq sequencing. The aim of this study was to (1) investigate the response of the entire microbial community to an increase in methane abundance, (2) identify types of MOB involved in the oxidation of methane, (3) test for the presence of MOB in natural seawater and sea ice communities and (4) relate these community features to methane oxidation rates.

2 Methods

2.1 Study site

30 Samples were collected at two sites between 7 April 2016 and 15 April 2016 in the Beaufort Sea (Table 1). Site "Elson Lagoon" (EL) is located north of Utqiagvik, Alaska, (7.4.2016, 71.334° N, -156.363° W). At the time of sampling EL was covered with 1.5 m thick sea ice; at approx. 1.5 m water depth, this left only a narrow layer of water between the sea ice and

the sediment. Site "Ice Mass Balance Buoy" (IMB) is located 1 km offshore of Utqiagvik, close to the ice mass balance buoy of the sea ice physics group of University of Alaska, Fairbanks (7.4.2016, 71.373° N, -156.548° W, and 9.4.2016, 71.372° N, -156.540° W). This site was characterized by 1 m thick fast ice cover and a water depth of approximately 7 m.

2.2 Sampling and instrument deployment

5 Seawater temperature and salinity records were taken with an YSI Professional Plus probe (YSI, Ohio, USA) and a YSI 600 OMS V2 sonde (YSI, Ohio, USA). Water was collected using either a peristaltic pump (Masterflex Environmental Sampler, Cole Parmer, Illinois, USA) or submersible pump (Cyclone, Proactive Environmental Products, Florida, USA) from different water depths. For determination of methane concentration and isotope ratios, water samples were collected as described in Uhlig and Loose (2017). Briefly, in the field, 0.7-0.9 L seawater was transferred bubble-free directly into in foil sample bags

10 (# 22950, Restek, Pennsylvania, USA). On return to the laboratory, a 0.1 L headspace of Ultra-High Purity nitrogen (Air Liquide, Anchorage, AK) was introduced into the bags through the septa, and the samples were equilibrated at 30°C for in situ measurements for at least 6 h.

For DNA extractions, between 1–2 L of seawater were filtered onto Sterivex® filter cartridges (Millipore) with 0.2 μM PES filter membranes directly in the field, or were filled into foldable polypropylene containers and filtered upon return to the

15 laboratory. For nutrient analysis an aliquot of the flow-through of the Sterivex® filters was collected in 15 mL polypropylene tubes (Falcon Brand, Corning, New York, USA) and frozen at -80°C. Seawater was fixed with 2% final concentration formaldehyde (Mallinckrodt Chemicals, Surrey, UK) and stored at 5°C to for later determination of the cell abundance.

Additionally, at site IMB, seawater temperature, salinity and velocities were recorded with an Aquadopp Profiler (Nortek

20 AS, Norway), and a salinity temperature recorder (SBE37SMP, Sea-Bird Scientific, Washington, USA). These were deployed at about 7 m depth on the seafloor between 9 and 15 April.

Sea ice was collected at site IMB only, using a Kovacs Mark II ice corer (Kovacs, Roseburg, Oregon, USA). The ice cores were sectioned into 15 cm and split lengthwise. The outside was cleaned with a sterilized knife to remove microbes possibly transferred from the sampling equipment. The core sections were sealed into custom-made gas-tight tubes (Loose et al.,

25 2011) for determination of methane concentration and isotope ratios. In the laboratory, the gas-tight tubes were flushed with ultrapure nitrogen for several gas volumes (Lorenson and Kvenvolden, 1995). Due to technical limitations, ice core 1 (IC1) was melted within a week at 5°C, while ice core 2 (IC2) was melted within a day, while frequently being mixed, at room temperature. Samples for molecular biology and cell counts were collected from the melted sea ice similar to the procedure described for seawater. In addition, the bottom 2 cm of one ice core was sampled into a sterile sample bag (Whirlpak, Nasco,

30 Fort Atkinson, WI, USA) for molecular biology processing only. Sea ice brine volume fractions were calculated according to Cox and Weeks (1983).

2.3 Net methane oxidation/production and determination of isotope fractionation factors

Rates for net methane oxidation/production were determined from the methane mass balance according to Uhlig and Loose (2017). In short, seawater was sampled into multi-layer foil bags. In addition to a headspace of hydrocarbon-free air (Air Liquide, Anchorage, AK), some sampling bags were supplied with a spike of methane. Final dissolved methane concentrations ranged between 3.0 and 4000 nmol L^{-1}, representing approximately 0.2x (no methane addition, resulting in degassing of in situ methane to the headspace), 2x, 10x and 200x of the in situ methane concentration. Samples were incubated at 0-1°C for 5 to 46 days. Some variation in the incubation period was introduced by logistical constraints. To account for potential diffusive loss of methane, a killed control was prepared for the 200x treatment by adding 0.1M NaOH. Assuming first order kinetics for oxidation of methane (Reeburgh et al., 1991; Valentine et al., 2001), net oxidation/production rate constants (k_{ox}) were determined from the methane mass balance in the incubations (Uhlig and Loose, 2017) as

$$\ln\left(\frac{n(CH_4)_{total, t_i}}{n(CH_4)_{total, t_{i-1}}}\right) = -k_{ox,ppm} \times t_{i-(i-1)} \tag{1}$$

with $n(CH_4)_{total,\ t_i}$ being the total molar mass of methane in the bag at time t_i.

The net oxidation/production rate (r_{ox}) was calculated from the first order constant and the in situ concentration of methane in the water:

$$r_{ox} = k_{ox} \times c(CH_4)_{w,\ in\ situ} \tag{2}$$

Isotopic fractionation factors of methane oxidation ($\alpha_{ox} = \frac{k_{12}}{k_{13}}$) were determined as described in Preuss et al. (2013), using the isotope fractionation approach (Coleman et al., 1981).

$$\ln\left(\frac{c(CH_{4ti})}{c(CH_{4t0})}\right)\left(\frac{1}{\alpha_{ox}} - 1\right) = \ln\left(\frac{1000 + \delta^{13}CH_{4ti}}{1000 + \delta^{13}CH_{4t0}}\right) \tag{3}$$

where the isotope ratios are described in δ-notation $\delta^{13}C = \frac{R_{sample}}{R_{standard}} - 1$, and R is the isotope ratio of $^{13}CH_4/^{12}CH_4$ in the sample and standard (VPDB, Vienna Peedee Belemnite, McKinney et al., 1950), respectively.

Alpha can be determined as $\alpha_{ox} = \frac{1}{m+1}$ from the slope (m) of the linear regression between $ln\left(\frac{c(CH_{4ti})}{c(CH_{4t0})}\right)$ and $\ln\left(\frac{1000 + \delta^{13}CH_{4ti}}{1000 + \delta^{13}CH_{4t0}}\right)$.

2.3 Analytical procedures

2.3.1 Methane concentration and stable isotope ratios

Methane concentrations and stable isotope ratios were determined with a Picarro G2201-*i* cavity ring-down spectrometer (Picarro, Santa Clara, California, USA) coupled to a Small Sample Isotope Module (SSIM) as described by Uhlig and Loose (2017). After equilibration, the headspace above the seawater or melted ice was subsampled with a gas tight syringe and 1 to

15 mL was injected into the SSIM. Measurements were performed in fast measurement mode. Dissolved methane concentrations were calculated as described in Magen et al. (2014), with the equilibrium constant according to Yamamoto et al. (1976).

2.3.2 Nutrient analysis and flow cytometry

5   Phosphate, nitrate and nitrite concentrations were determined using a QuickChem QC8500 automated ion analyzer (Lachat, Loveland, Colorado, USA). The total number of prokaryotic cells was counted on a BD Influx[TM] flow cytometer with BD FACS[TM] software. Formol-fixed samples were stained with a final concentration of 1x SYBR Green I (Invitrogen, Molecular Probes, Eugene, Oregon, USA) for 20 to 45 min at room temperature in the dark before analysis.

2.4 Nucleic acid extraction and sequencing

10   DNA was extracted with the PowerWater® DNA extraction kit (MoBio, Carlsbad, California, USA). To remove the filter membrane, the Sterivex® cartridge was opened with a pair of sterilized pliers. The filter membrane was cut out along the edge with a scalpel, transferred into the bead tube, and DNA subsequently extracted according to the manufacturer's protocol. A minor modification was made: the tube was vortexed once for 3 minutes, rotated 180°, and then vortexed for another 3 minutes. The DNA was eluted in 80 µL buffer PW6, after incubating the buffer for 1 min on the membrane.

15   Quantification was conducted with a Qubit®2.0 Fluorometer (Invitrogen, Carlsbad, California, USA).

The V4-V5 region of the 16S rRNA gene was amplified with forward primer 518F (5´-xx-CCAGCAGCYGCGGTAAN-3´), and an 8:1:1 mix of the reverse primers 926R1 (5´-yy-CCGTCAATTCNTTTRAGT-3´), R2 (5´-yy-CCGTCAATTTCTTTGAGT-3´) and R3 (5´-yy-CCGTCTATTCCTTTGANT-3´) (Nelson et al., 2014). Primers included 33 base pair (bp) adapters (xx, yy) at the 5´end. The final volume of 20 µL PCR reaction contained 0.2 µL PfuUltra II fusion

20 HS DNA polymerase (Agilent Technologies, Santa Clara, California, USA), 50 µM each forward and reverse primer, 25 µM each dNTPs (Thermo Scientific, Waltham, Massachusetts, USA), 10 µg mL^{-1} BSA (Thermo Scientific, Waltham, Massachusetts, USA) and 1 ng template DNA. After initial denaturation for 2 min at 95°C, DNA was amplified in 30 cycles of 30 seconds 95°C denaturation, 30 seconds 55°C annealing and 30 seconds at 72°C for extension, with a final extension of 2 minutes at 72°C. The *pmoA* subunit of the particulate monooxygenase (pMMO) was amplified with primer pair 189f (5´-

25 xx-GGNGACTGGGACTTCTGG-3´) and mb661r (5´-yy-CCGGMGCAACGTCYTTACC-3´) (Holmes et al., 1999; Lyew and Guiot, 2003). The PCR conditions were the same as described for the V4-V5 amplicon. All amplicons were purified with Agencourt® AMPure® XP magnetic beads (BeckmanCoulter, Indianapolis, Indiana, USA) at a ratio of 0.7x bead solution per PCR reaction volume and washed with 80% ethanol.

The primer sequences specified above included adapter sequences (xx, yy) to attach Nextera indices and adapters in a second

30 PCR reaction of 6 cycles with 50 ng template DNA (http://web.uri.edu/gsc/next-generation-sequencing/). Amplicons were sequenced with Illumina MiSeq at 2x250 bp read length.

2.5 Sequence analysis

2.5.1 V4-V5 region of 16S rRNA gene

Demultiplexing and adapter removal was performed with Illumina software. V4-V5 sequence quality control and clustering was performed in mothur (Schloss et al., 2009) as follows. Contigs were prepared from forward and reverse reads and culled if they contained ambiguous bases or homopolymers longer than 6 bases. Contaminating sequences observed in kit and filter blanks accounted for 1.4% of all sequences and were removed from all samples. After alignment to the Silva small subunit reference database (v123; Quast et al., 2013), the 408 bp long sequences were preclustered (1% variability allowed) and filtered for chimeras (de novo algorithm) with the UCHIME (Edgar et al., 2011) wrapper in mothur. Sequences identified as chloroplast, mitochondria, Archaea, Eukaryota or unknown were removed and operational taxonomical unit (OTUs were built at a 3% distance level with the opticlust algorithm. OTUs with fewer than 2 reads were removed from further analysis. Visualization and further analysis of sequencing data was performed in R version 3.2.3 (R CoreTeam, 2015) in RStudio Version 0.99.903. Species diversity was analyzed using the phyloseq package (McMurdie and Holmes, 2013) to determine richness (Shannon and Simpson indices) and differences in community structures (Bray-Curtis dissimilarities). Differences in community structure associated with different methane spike concentrations were determined via analysis of similarity (ANOSIM) in the package vegan (Oksanen et al., 2017) on three predefined groups: in situ (N=9), 0.2x (N=2) and 10x (N=3). Groups 1x, 200x short, 200x long with N=1 (Table 2), were excluded from the analysis.

2.5.2 Identifying potential methane-oxidizing bacteria

To select groups representing methylotrophs and methanotrophs, 16S OTUs were filtered according to their phylogenetic annotation assigned by mothur for containing the string "meth" on family, order and genus level. This filter is expected to find 97% of taxonomically annotated methanotrophs, according to a current review on the diversity of methanotrophs (Knief, 2015).

Further, phylogenetic groups potentially involved into methane cycling were identified as differentially more abundant 16S OTUs between incubations (0.2x, 10x, 200x) and in situ samples using DESeq2 (Love et al., 2014). Only OTUs with an adjusted p-value in DESeq2 < 0.05 were kept for further analysis. OTUs identified from spike 0.2x were considered to represent groups favored due to the incubations (the "bottle effect") rather than addition of methane, and removed from further analysis. Treatments EL 0.2x, EL 10x and IMB 2x (Table 2) were not included in this analysis, since no replicate samples were available. The abundance of all candidate 16S OTUs, identified as described above, was determined within every in situ or incubated sample.

Absolute numbers of methanotrophs and methylotrophs were calculated by multiplying the relative 16S sequence abundance with flow cytometric cell counts. The absolute numbers were further corrected for the mean of the 16S gene copy number for the lowest taxonomic rank (class to genus) available in the rrnDB-database (Stoddard et al., 2015).

2.5.3 Particulate methane monooxygenase: *pmoA*

In addition to 16S genes, the alpha subunit of the particulate methane monooxygenase (*pmoA*) was used as molecular marker for MOB. Only *pmoA* forward reads were analyzed. High-quality *pmoA* reads were retrieved according to the following protocol. Using mothur (Schloss et al., 2009), all reads were trimmed to a length of 225 bp to remove sequence fractions with a mean quality score below 30 (fastqc; Andrews, 2010). In addition, reads were clipped whenever the average quality score over a 50 bp window dropped below 30. Sequences with ambiguous bases and homopolymers larger than 6 bp were culled. Only sequences that translated into uninterrupted protein reading frames (Emboss 6.60 / transseq; Rice et al., 2000) were kept for further analysis. Nucleic acid sequences were aligned to a reference dataset of *pmoA* sequences (fungene; Fish et al., 2013) and sequences of a length of at least 220 bp were preclustered (1% variability allowed). De novo chimera filtration was run with the UCHIME (Edgar et al., 2011) wrapper in mothur. A similarity of 93% between *pmoA* sequences was defined to match the 97% cutoff as species definition for the 16S gene (Lüke and Frenzel, 2011). *PmoA* OTUs were built at a maximal distance of 7% between the furthest neighbors to maximize resolution between OTUs due to the short read length and limited number of unique sequences (Supplementary Table 1). To determine the phylogenetic relationship of *pmoA* sequences, nucleotide sequences were aligned against selected reference sequences in Mafft 7.017 (Katoh and Standley, 2013) and a neighbor joining tree calculated in Clustal 2.1 (Larkin et al., 2007) with 1000 replications.

3 Results

3.1 Water column properties

On 7 April 2016, the narrow layer of water between the sediment and ice in Elson Lagoon (N=1) had a salinity of 21 and a temperature of -1.5°C. Phosphate and nitrate concentrations were 0.74 µM and 4.87 µM, respectively. Methane concentration for Elson Lagoon (N=1) was 53.2 nmol L^{-1} with a stable isotope ratio of -73.8 ‰ (Figure 1) and cell density 7.7 x 10^4 cells mL^{-1}. For most days during the sampling period, the water column at station IMB was characterized by temperatures around -1.8°C and salinities of 33.9 to 36.4 (Figure 1, Supplementary Figure 1, 2). Between 11 April and 13 April warmer water (max. temperature observed -0.9°C) was advected, coinciding with a change in current direction. A lower salinity of 27.5 at the ice-water interface indicates melting of the sea ice. Phosphate concentrations at station IMB were 0.99 ± 0.33 µM (N=9) and nitrate 6.59 ± 4.04 µM (N=9), with neither showing any trends in the depth profiles (data not shown). Nitrite concentrations were below detection (0.3 µM based on technical replicates). Water column methane concentrations at station IMB ranged between 9.2 and 25.3 nmol L^{-1} (16.3 ± 7.2, N=5) (Figure 1), with stable isotope signatures between -55.4 and -70.5 ‰ (-60.6 ± 6.3, N=5)). Total prokaryotic cell densities, determined as SYBR Green stained cells with flow cytometry, were 6.9 x 10^4 ± 5.7 x 10^3 cells mL^{-1} (N=16).

3.2 Ice cores

Temperature and salinity profiles of the two sea ice cores sampled at 9 and 15 April are shown in Figure 2. Brine volume fractions above 5% indicate that the ice was permeable for water and gases (Golden et al., 1998) in the bottom 50–100 cm, while the upper part of the ice was impermeable. Methane concentrations in the ice were higher than in the water (83.9 nmol kg^{-1} ± 35.0 nmol kg^{-1}, N=9) while the isotope signatures were close to seawater (-60.4‰ ± 3.5‰, N=9). Ice core 1 (IC1), sampled on 7 April, had generally higher methane concentrations and isotope signatures (72.3 nmol kg^{-1} to 144.3 nmol kg^{-1}, -54.4‰ to -62.0‰) than ice core 2 (IC2), sampled on 15 April (53.3 nmol kg^{-1} to 77.6 nmol kg^{-1}, -59.0‰ to -61.6‰). Microbial activity during storage of IC1 at 5°C for one week before analysis might have led to the differences in methane concentrations and isotope ratios. For ice samples, cell counts were performed on IC2 only; they show an increase from 1.0 x 10^4 cells mL^{-1} in the top layers to 8.2 x 10^5 cells mL^{-1} in the bottom two cm of the ice core.

3.3 Net methane oxidation/production and isotope fractionation

The methane oxidation potential of microbial seawater communities at stations EL and IMB was determined from the methane mass balance in incubation experiments (Table 3; Uhlig and Loose, 2017). Final dissolved methane concentrations ranged between 3.0 and 4000 nmol L^{-1}, representing approximately 0.2x to 200x the in situ concentration. Oxygen concentrations at the end of the long incubations ranged between 116% and 126% saturation, while oxygen concentrations at the end of the short incubations were not determined.

Net oxidation rates discussed here were published in Uhlig and Loose (2017) and are summarized for comparison with the microbial community structure. Short incubations (≤10 days) did not show significant oxidation, while long-term incubations (41–46 days) did. Surprisingly, four out of five replicates of treatment 0.2x IMB showed a statistically significant increase in methane of about 0.62 ± 0.21 nmol L^{-1} (N=5) within 10 days (Supplementary Figure 3). In long-incubation samples with significant methane oxidation (10x and 200x spikes), the isotopic signature of the residual methane increased toward heavier (more positive) signatures with fractionation factors α of 1.0230 (10x EL), 1.0225 (10x IMB) and 1.0103 (200x IMB).

3.4 Bacterial community structure

The V4-V5 region of the 16S rRNA gene was sequenced from a total of 10 seawater samples and 7 ice samples (Table 2). Non-metric multidimensional scaling analysis of the Bray-Curtis diversity revealed high similarity across the in situ water samples analyzed for 16S diversity (Figure 4). Samples from site IMB clustered together repeatedly, and we did not observe any differences in community structure coinciding with water depth or temperature (Figure 4). For the IMB samples, IMB 2 was the only sample slightly different from the other in situ samples, though IMB 1, IMB 2, IMB 4 are all characterized by a colder water mass. Only IMB3 showed some influence of an incoming warm water mass in the YSI profile (Figure 1), though not yet reaching the bottom (Supplementary Figure 1), but this shift is not seen in the community structure. In contrast to the in situ water samples, the community structure of incubated samples is driven by incubation time. While

communities in the short-incubation treatments (5–10 days; 0.2x, 2x, 200x short) were similar to the in situ samples, the long incubations (41–46 days; 10x, 200x long) clearly deviated from the in situ samples. In both the long and short incubated clusters samples originating from IMB 1 (0.2x, 10x) and IMB 2 (2x, 200x) are present (Figure 4, Table 2). Microbial communities in ice cores were clearly distinct from those in the water samples and were more distant to each other than were the communities in water samples.

In the in situ seawater communities, Proteobacteria were dominant with relative sequence abundances of 59.5% and 65.5% ± 2.5 % for EL (N=1) and IMB (N=9), respectively (Supplementary Figure 4). Within the phylum of Proteobaceteria, α- and γ-Proteobacteria made up the majority. The second most abundant phylum was Bacteriodetes with 23% and 19.6% ± 1.4% for EL and IMB, respectively.

Similar to the seawater, sea ice (N=7) showed a dominance in Proteobacteria (58.9% ± 9.8%), but Bacteriodetes sequences (29.1% ± 11.7%) were slightly more abundant in the ice than in the water. γ-Proteobacteria dominated in all but one sample (IC2 30–46 cm). This one sample, which had clearly visible sediment included into the sea ice structure, was dominated by α-Proteobacteria.

In all incubated samples that were sequenced (N=10), species richness decreased (Figure 3) and the communities shifted toward higher fractions of γ-Proteobacteria over time. In short incubations (5–10 days; N=5) γ-Proteobacteria dominated with 61.8% ± 2.9% of sequences, while reaching 81.0% ± 11.1% in long-incubation samples (41–46 days; N=4). In particular, one operational taxonomical unit (OTU), from the genus *Oleispira*, was very abundant in the long-incubation samples, with 50.1 to 76.3%, compared to abundances <0.04% in the in situ samples. The same OTU was only slightly more abundant in the short-incubation treatments (0.5%–1.6%) compared to in situ abundances. In addition to the shift in community structure, total cell densities increased to 1.9 x 10^5 and 3.3 x 10^6 cells mL^{-1} for short and long incubations, respectively, based on flow cytometric cell counts.

3.5 Methanotrophs, methylotrophs and differentially abundant OTUs

Using their 16S taxonomic annotation, we identified six groups of aerobic methanotrophs (MOB) (Figure 5). With a maximum of 1.76% ± 0.73%, the relative abundance of MOB was low in all samples (Table 4). Four MOB grouped in the Methylococcales (γ-Proteobacteria), specifically Marine Methylotrophic Group 1 and 2 (MMG1, MMG2), unclassified Methylococcales and the Milano-WF1B-03 family. The three remaining MOB OTUs belonged to the genera *Methylobacterium* and *Methyloceanibacter* (α-Proteobacteria) and *Candidatus "Methylacidiphilum"* (Verrucomicrobia). MOB OTUs were more abundant in natural seawater samples than in sea ice (maximal 0.11% in IC1 0–16 cm), but in contrast to the seawater, α-Proteobacteria MOB dominated in the sea ice.

Furthermore, four clades of non-methane utilizing methylotrophs (non-MOB methylotrophs) were identified, grouping into γ-Proteobacteria Marine Methylotrophic Group 3 (MMG3) and *Methylophaga*, and to the β-Proteobacteria Methylophilaceae (*Methylotenera*, OM43 clade). Non-MOB methylotroph OTUs were more abundant than MOB OTUs with exception of the 200x incubation treatments (Figure 5, Table 4). Ice samples showed the largest difference in abundance between non-MOB

methylotrophs and MOB, with a ratio of 21:1 between the two groups. Ice samples also had the highest overall relative abundance of methylotrophs (MOB and non-MOB) of all in situ samples (max: 1.63%, IC1 0–16 cm). Only the 200x long incubations had a higher total number of methylotrophs (3.3%), while this sample was in addition dominated by MOB (2.49%). The second highest relative abundance of MOB was found for in situ EL and IMB with 0.24% ± 0.09% (N=10).

Taking into account the total cell number, a strong increase of MOB groups MMG1 (2 to 700 times) and Milano-WF1B-03 (25 to 75 times) was observed for the 10x and 200x long-incubation samples compared to in situ conditions (Figure 5b).

Taxonomic groups that became differentially more abundant in the incubated samples than in natural communities were the γ-Proteobacteria *Oleispira*, *Colwellia* and *Glaciecola,* as well as Rhodobacteracea (α-Proteobacteria). Except for *Oleispira*, which became dominant, the other taxa had relative sequence read abundances from 1.1% to 12.6% after the oxidation experiments, compared to abundances <0.25% for in situ samples (Supplementary Figure 5).

3.6 Particulate methane monooxygenase (*pmoA*) sequences

A 225 base pair section of the particulate methane monooxgenase gene (*pmoA*) was sequenced in a total of 15 samples (Table 2). The absolute abundance of *pmoA* fragments obtained in sequences ranged from 9331 (IMB in situ, 6.5 m depth) to 72781 (IMB 200x long) reads. In general, incubations with higher methane concentration had more *pmoA* reads than incubations with lower methane concentration or in situ samples. About three times more reads were filtered from the Elson Lagoon in situ sample (33844 reads, N=1) than the IMB in situ samples (11700 ± 1833, N=4).

Two of the 59 *pmoA* OTUs made up 96.8% of all sequences, while all other OTUs individually represented ≤1% of the *pmoA* sequences. The most abundant OTU (71.0% of all sequences) clustered with two uncultured isolates from methane seeps (NCBI accession: HQ738559, EU444875) in the deep sea-3/OPU3 subgroup of γ-Proteobacteria Type I MOB (Hansman et al., 2017; Knief, 2015; Lüke and Frenzel, 2011). The second most abundant (25.8%) OTU was related to *Methyloprofundus sedimentii*, another Type I MOB. Most of the low-abundance OTUs also clustered within the Type I MOB, while only three OTUs (0.07% of all *pmoA* sequences) clustered with Type II α-Proteobacteria MOB *pmoA* sequences (*Methylocystis*, *Methylosinus*).

4 Discussion

4.1 Methane concentration and stable isotope ratios in seawater and ice

Seawater methane concentrations in April 2016 close to Utqiagvik Alaska were supersaturated 250% to 700% compared to atmospheric equilibrium (3.6 nmol L^{-1}). The concentration at site EL (52.90 nmol L^{-1}, N=1, 7.4.2016) was in the range of a study by Lecher et al. (2016) in Elson Lagoon under ice free conditions (3.3–124.0 nmol L^{-1}). At site IMB, concentrations were slightly lower (9.5 nmol L^{-1} – 25.2 nmol L^{-1}: N=5, 15.4.2018) than previously reported from the same area for ice free (Lecher et al., 2016; mean: 40.6 nmol L-1), and ice covered conditions (Zhou et al., 2014; March/April: 37.5 ± 6 nmol L-1). Shallower depths at IMB exhibit lower methane concentrations (Figure 2), and the isotopic signature mirrors this pattern

with more positive values toward the surface. This indicates that methane might be biologically oxidized on the way through the water column, after being released from the sediment.

The sea ice bulk methane concentrations observed in this study (53–144 nmol kg^{-1}) are significantly higher than in a study from the same area (Zhou et al., 2014), but fall within values reported for the Beaufort Sea (5 - 1260 nM, Lorenson and Kvenvolden, 1995). Methane carbon isotopic signatures (-54.4 to -63.8 ‰) are comparable to the higher end of previous studies for bulk sea ice (-52.1‰ to -83.4‰, Lorenson and Kvenvolden, 1995) and sea ice brine (-75‰, Damm et al., 2015). Although both ice cores were sampled within 300 m distance from each other at site IMB, they differ in concentration and isotope signature. These differences could either be caused by spatial variability between the two ice cores or differences in the processing procedure described in section 2.2. Spatial variability as driving difference between the two ice cores is corroborated by the sediment present at 30–46 cm depth in IC1, which was not observed in IC2, indicating that both ice cores have different freezing histories. The same event that led to inclusion of the sediment into IC1 possibly resulted in inclusion of higher methane concentrations into IC1 compared to IC2 during freeze-up. In addition, microbial processes like oxidation of methane or methanogenesis could have taken place in situ or during sample processing and storage. Microbial oxidation of methane, particularly in the two middle sections (30-46 cm and 52-86 cm depth), might have led to the observed shift toward more positive carbon isotope ratios (Figure 2). The different bacterial community introduced through the sediment (Supplementary Figure 4) might have favored oxidation in those two sections compared to the top and bottom sections. MOB identified by our approach were, however, neither more abundant nor phylogenetically distinct in the sediment-loaded section compared to the other sections (Figure 4a). Another microbial process that may have led to the discrepancies between IC1 and IC2 could be methane production from ice algae-derived organic carbon in IC1. With typical carbon isotopic signatures of -20‰ to -30‰ for ice-derived carbon (e.g. Wang et al., 2014), methane produced from this substrate would be enriched in ^{13}C (more positive) compared to the initial pool of methane (about -60‰, Figure 2, Figure 6). Yet, sequences of bacterial taxa that might indicate anoxic conditions (Eronen-Rasimus et al., 2017), which would favor anaerobic methane production, were not significantly more abundant in IC1 than in IC2 (Supplementary Table 2).

Compared to the underlying water column, methane concentrations in the sea ice were two to five times higher. Further, the isotope signatures indicate less oxidized methane (-60.4 to -63.8 ‰) in most of the ice sections compared to the upper water column (-55%). Lorenson and Kvenvolden (1995) report higher methane concentrations in sea ice than in the water column for the Beaufort Sea. They attributed the high methane concentrations in the fast ice to inclusion of sediment-sourced methane during the initial freeze-up over the shallow shelf at <10 m water depth (Lorenson et al., 2016). Methane concentrations in IC2, which are close to water column concentrations reported in previous studies for the Barrow shelf (Lecher et al., 2016; Zhou et al., 2014), suggest the same process for our ice cores. Further, in our study, the lower methane concentrations together with more positive (heavier) isotopic signature in sea water compared to ice, might indicate that the microbial community in the water column is oxidizing more methane during the ice covered period than in the freeze-up period. Higher oxidation rates during ice covered periods compared to ice free conditions were previously reported for the

Beaufort Sea. Due to reduced sea-air gas exchange, higher methane concentrations can build up under sea ice cover, which might lead to higher oxidation rates (Lorenson and Kvenvolden, 1995).

4.2 Methane cycling at different methane concentrations

Net methane oxidation/production rates were determined from water sampled at station IMB 1 and IMB 2 on 7 and 9 April
5   2016. Both days were characterized by the cold water temperatures ($\leq$-1.8°C; Fig. 1). Different water masses have previously been reported to influence the methane oxidation potential of water column microbial communities off Svalbard (Steinle et al., 2015). In this study, we observed a change in current direction and water temperature consistent with advection of a different water mass into the study area (Supplementary Fig. 1). However, this change occurred on 12 April subsequent to sampling IMB 3, and thus this event would not have influenced the net oxidation potential determined in this
10   study.

Net oxidation rates of the long-incubation treatments at 10x (46 days) and 200x (41 days) methane concentration fall into the mid-range of rates published for Arctic and subarctic environments (Damm et al., 2015; Gentz et al., 2014; Lorenson et al., 2016; Mau et al., 2013, 2017; Steinle et al., 2015) or marine sites with high oxidation rates at oil spills or gas flares (Redmond et al., 2010; Valentine et al., 2010), as discussed in Uhlig and Loose (2017). The fractionation factors (α_{ox}) that
15   we observed are higher than previously reported from cold marine environments with a range of α_{ox} from 1.002 to 1.017 (Cowen et al., 2002; Damm et al., 2008; Grant and Whiticar, 2002; Heeschen et al., 2004; Keir et al., 2009; Tsunogai et al., 2000). Some of these fractionation factors, which were calculated from in situ data, might however be underestimates due to mixing effects in the water column (Grant and Whiticar, 2002). The fractionation factors in our study seem to be inversely dependent on the methane spike concentration, with higher fractionation in the 50x (1.023, N=6) treatments than in the 200x
20   (1.010, N=2) treatments. The relative and absolute abundances of MOB, as well as the dominant MOB types, differed between both treatments, possibly providing explanations of the differences in fractionation rates. Logistical constraints forced us to stop several incubations already after 5 to 6 days. These short-incubation 2x and 200x treatments did not resolve oxidation of methane. While the 2x treatments did not meet the sensitivity threshold for the method (Uhlig and Loose, 2017), the 200x short treatments were likely just about to leave the lag phase when the experiments were stopped. A lag phase of 6
25   days was observed for the long-incubation 200x samples, in which the microbial community possibly to shifted toward an abundance of MOB that was large enough to cause detectable methane oxidation. To facilitate comparisons between treatments, incubation duration should be kept constant in future studies.

The increase in methane concentration in treatment IMB 0.2x (10 days incubation) is surprising since experiments were performed under aerobic conditions. Since the seawater was not pre-filtered through a larger pore-size filter, which would
30   exclude larger particles but allow bacterial cells to pass, production of methane in microanoxic zones (de Angelis and Lee, 1994; Oremland, 1979) should be considered. Furthermore, several studies suggested pathways for methane production in oxygenated marine systems from methylated compounds or dissolved organic matter (Damm et al., 2010; Florez-Leiva et al., 2010; Karl et al., 2008; Repeta et al., 2016). The methane production rate of 0.06 nmol L^{-1} day^{-1} observed in our study is two

to six orders of magnitude lower than previously published methane production rates under aerobic conditions (Damm et al., 2010; Karl et al., 2008). In addition to biological processes, we cannot rule out an abiotic effect leading to the increased methane concentrations, since our experimental setup did not include a killed control at the same methane concentration.

4.3 Abundances of MOB and non-MOB methylotrophs control the methane oxidation potential

5   We found a strong linear correlation between the net oxidation rate constant (k_{ox}) and the relative abundance of 16S MOB sequences (Spearman rank order coefficient $\rho_s = 0.79$, p=0.006) (Figure 7a, Table 5). This strong correlation is confirmed when correlating against the total abundance or DESeq2 normalized abundance of 16S MOB sequences (Table 5). The correlation to k_{ox} is even stronger for the absolute abundance of *pmoA* sequences retrieved from the respective datasets ($\rho_s = 0.86$, p=0.006) (Figure 7b). This presentation of a direct and statistically significant linear relationship is the first to our
10 knowledge. It agrees with other qualitative reports of positive correlations between methane oxidation rates and abundance of *pmoA* or MOB 16S rRNA genes determined using a variety of methods - quantitative PCR, FISH, or sequencing - for marine water column and lake sediments (Crespo-Medina et al., 2014; Deutzmann et al., 2011; e.g. Rahalkar et al., 2009; Steinle et al., 2015). Future application of marine-specific *pmoA* primers may further improve this correlation (Tavormina et al., 2008).

15 Cell-specific net oxidation rates in our study (3.2–7.5 fmol cell^{-1} h^{-1}) were relatively constant between treatments. They are two orders of magnitude higher than reported for subarctic sea water (Steinle et al., 2016). Since the cell-specific rates only span a narrow range, the ultimate control on the methane oxidation potential is the number of MOB.

Despite the long incubation time in our experiments and the fact that methane was the only added source of carbon, the relative abundance of MOB determined from 16S reads was low (<2.5%, Table 4). Other studies of natural or man-made gas
20 or oil spills, with dissolved methane concentrations comparably high to our 10x and 200x treatments, reported maximal values of 8 to 34% of MOB (Crespo-Medina et al., 2014; Kessler et al., 2011; Steinle et al., 2015, 2016). Surprisingly, relative sequence abundances of MOB in the natural seawater communities were higher than in the incubations except for the 200x treatment (Table 4). Inferred absolute MOB numbers were higher in 10x and 200x incubations than in situ (Figure 5b). In contrast, absolute MOB numbers in 0.2x and 2x incubations were very similar to in situ abundances, indicating that
25 either the provided methane concentration was too low or the incubation time too short to stimulate MOB growth.

It is puzzling why the fraction of methane oxidizers in the bacterial community did not increase above the observed low percentages although the cell-specific oxidation rates were high and sufficient methane was available, particularly in the 10x and 200x treatments. Oxygen and methane can be ruled out as limiting factors, since both were abundant. Copper, which is essential for expression of particulate methane monooxygenase, can restrict MOB growth (Avdeeva and Gvozdev, 2017;
30 Zhivotchenko et al., 1995). In the absence of copper, many MOB express a copper-independent soluble methane monooxygenase (Hakemian and Rosenzweig, 2007). Since we did neither determine copper concentrations, nor the expression of particulate and soluble methane monooxygenase, we cannot exclude that copper was limiting in our study. Further, the low relative abundance of MOB sequences could be due to competition with other bacterial taxa for other

macro- or micronutrients. In the absence of other added C substrates, these other taxa could have utilized the initial pool of dissolved organic carbon (DOC). DOC concentration is about 68 μM carbon in the Southern Chukchi Sea (Tanaka et al., 2016), which is in the same range as the amount of consumed methane carbon in the 200x treatments and two orders of magnitude higher than the consumed carbon in the 10x treatments.

5   As a result of the low MOB abundances, the potential of the microbial community to mitigate release of dissolved methane to the atmosphere by oxidation is small. For example, for methane concentrations in the Laptev Sea area, the rates observed in this study would result in 0.2% consumption during the ice covered period. This supports the results from a previous study for the Beaufort Sea, where 1–2% of dissolved methane was calculated to be oxidized (Lorenson et al., 2016).

4.4 Structure of the methane degrading microbial community

10   This first 16S MiSeq sequencing based study on methane-oxidizing sea water communities in the Arctic provides a broader view on the community structure than approaches with FISH and DGGE. The dominance of γ-Proteobacteria MOB in our natural and incubated seawater samples agrees with previous records of MOB diversity for polar and subpolar waters (Mau et al., 2013; Steinle et al., 2015; Verdugo et al., 2016). In addition, non-methane-utilizing methylotrophs were present in all of our samples. The relative read abundance of non-MOB methylotrophs were, similar to MOB, tightly correlated to k_{ox}, and

15   the same correlation holds for the relative abundance of total methylotrophs (MOB plus non-MOB). In contrast, the correlation between OTUs that were differentially more abundant in the incubated samples and k_{ox} was weak (Table 5). This points toward a possible link between the MOB and non-MOB in this methane-oxidizing microbial community, in which non-MOB methylotrophs might play a role for community methane oxidation, whereas the OTUs that were differentially more abundant, are not directly linked to methane oxidation.

20   Methylophilacaea, the most abundant non-MOB methylotroph in our experiments, have been found to be abundant in sediment methane-oxidizing communities in lakes and marine systems (Beck et al., 2013; Redmond et al., 2010). Possible cooperative behavior between methanotrophs (Methylococcaceae) and non-MOB methylotrophs (Methylophilaceae) was suggested (Beck et al., 2013), in which the latter cross-feeds on intermediate metabolic products of the MOB, i.e. methanol, and can even positively alter the metabolism of the MOB toward methane assimilation (Krause et al., 2017).

25   To test if the non-methane MOB could be supported by the intermediate substrates produced by MOB, we calculated a budget between the methane carbon assimilated by the growing microbial population ($C_{CH_4,assim}$), and the cell carbon gained during growth ($C_{cell-growth}$) (Figure 8). We assumed (i) a cellular carbon content of 150 fg for exponentially growing bacterial cells (Vrede et al., 2002) and (ii) that about 1/3 of consumed CH_4-carbon is assimilated, with the remaining 2/3 respired to CO_2 (Bastviken et al., 2003; Roslev et al., 1997). $C_{CH_4,assim}$ exceeds MOB-$C_{cell-growth}$ by a factor of 9 to 17,

30   indicating that some of the $C_{CH_4,assim}$ was available for secondary consumption by non-MOB. The entire methylotrophic community (MOB + non-MOB-methylotroph) growth can also be explained solely by $C_{CH_4,assim}$, supporting the possible link of non-MOB methylotrophs to methane consumption. In contrast, only about 0.1% of the total community growth could

be supported by $C_{CH_4,assim}$ in the 10x treatment and 15% in the 200x treatment. The remaining cell growth, e.g. of the differentially more abundant OTUs, must have been supported by other carbon sources, such as initially available DOC.

4.5 MOB and methylotrophs in sea ice

5   The two sea ice cores analyzed in this study give a first insight into the possible role of methane oxidizers in sea ice. In contrast to seawater samples, MOB found in sea ice samples were mostly α-Proteobacteria. The relative sequence read abundance of MOB in the ice was very low (maximal 0.1%), pointing to an overall low contribution of methane oxidation inside sea ice. The highest relative abundances of MOB were found in the top-most ice sections in both ice cores (Figure 5a). This coincided with the highest methane concentration in case of IC2, whereas the top-most section of IC1 had the second

10   smallest concentration of methane in this ice core (Figure 2e). Relative abundances of MOB in the inner and bottom sections of the ice cores were even lower, with 0 to 0.02% only.

The top-most section of IC1 and the biologically rich bottom section of IC2 had the highest relative abundances of β-Proteobacteria Methylophilaceae, a non-MOB methylotroph. Recently identified as DMS degraders (Eyice et al., 2015), Methylophilaceae might use DMS, a methylated compound abundant in sea ice, as substrate (Kirst et al., 1991).

15   ## 5 Conclusions

We studied the structure and methane oxidation potential of microbial communities from Arctic seawater and sea ice. The natural seawater community had relative sequence abundances of MOB of 0.24% ± 0.09% and was dominated by γ-Proteobacteria MOB, while α-Proteobacteria MOB dominated in sea ice with maximal fractions of ≤0.1% in the surface of the sea ice. In seawater incubations under different methane concentrations, the overall relative abundance of methane

20   oxidizers (MOB) was low, with a maximum of 2.5% and the dominant MOB types were γ-Proteobacteria. A tight correlation between the rate constant of methane oxidation and relative abundances of MOB and non-MOB methylotrophs (Figure 7, Table 5) suggests that the abundance of MOB is a control on the magnitude of methane oxidation. It also suggests that non-MOB methylotrophs might play a role in methane oxidation. The reasons for low MOB abundance, despite ample methane availability, along with the role of methylotrophs in methane oxidation are both open questions.

25   Higher methane concentrations in the sea ice compared to the underlying water and an offset in stable isotope ratios suggest that either fractionation and solute concentration occurred during freeze-up, or different microbial processes took place within the ice and water. Possible causes explaining this observation include (i) microbial production of methane, even within the ice (Damm et al., 2015), and (ii) microbial oxidation in the water column and at lower rates in sea ice. To address these hypotheses, future studies should directly compare both sea ice and water, particularly during ice freeze-up, and

30   involve investigation of the microbial processes.

Acknowledgements

This work was supported by the American Chemical Society, Petroleum Research Fund (PRF# 54473-DNI2). Part of this research is based upon work conducted using the NSF EPSCoR Marine Science Research Facility and the Rhode Island NSF EPSCoR Genomics and Sequencing Center, which are supported in part by the National Science Foundation under EPSCoR Grants Nos. 0554548 and EPS-1004057. We thank Clarisse Sullivan for support with preparations for fieldwork and Rodrigue Spinette for help with flow cytometry and qPCR as well as the nutrient measurements. We thank David C. Smith and Lucie Maranda for lending equipment and discussing concepts and experimental procedures. We thank Hajo Eicken, Joshua Jones and Andy Mahony from University Alaska Fairbanks for discussing the local oceanographic conditions.

References

Andrews, S.: FastQC: a quality control tool for high throughput sequence data. Available online at: http://www.bioinformatics.babraham.ac.uk/projects/fastqc (Accessed 29 September 2017), 2010.

de Angelis, M. A. and Lee, C.: Methane production during zooplankton grazing on marine phytoplankton, Limnol. Oceanogr., 39(6), 1298–1308, doi:10.4319/lo.1994.39.6.1298, 1994.

Avdeeva, L. and Gvozdev, R.: Effect of gopper goncentration on the growth of *Methylococcus gapsulatus* (Strain M), Chem. J. Mold., 12(1), 110–114, doi:10.19261/cjm.2017.404, 2017.Barnes, R. O. and Goldberg, E. D.: Methane production and consumption in anoxic marine sediments, Geology, 4(5), 297, doi:10.1130/0091-7613(1976)4<297:MPACIA>2.0.CO;2, 1976.

Bastviken, D., Ejlertsson, J., Sundh, I. and Tranvik, L.: Methane as a Source of Carbon and Energy for Lake Pelagic Food Webs, Ecology, 84(4), 969–981, 2003.

Beck, D. A. C., Kalyuzhnaya, M. G., Malfatti, S., Tringe, S., Glavina del Rio, T., Ivanova, N., Lidstrom, M. and Chistoserdova, L.: A metagenomic insight into freshwater methane-utilizing communities and evidence for cooperation between the *Methylococcaceae* and the *Methylophilaceae*, PeerJ, 1, e23, doi:10.7717/peerj.23, 2013.

Boetius, A. and Wenzhöfer, F.: Seafloor oxygen consumption fuelled by methane from cold seeps, Nat. Geosci., 6(9), 725–734, doi:10.1038/ngeo1926, 2013.

Coleman, D. D., Risatti, J. B. and Schoell, M.: Fractionation of carbon and hydrogen isotopes by methane-oxidizing bacteria, Geochim. Cosmochim. Acta, 45(7), 1033–1037, doi:10.1016/0016-7037(81)90129-0, 1981.

Cowen, J. P., Wen, X. and Popp, B. N.: Methane in aging hydrothermal plumes, Geochim. Cosmochim. Acta, 66(20), 3563–3571, doi:10.1016/S0016-7037(02)00975-4, 2002.

Cox, G. F. N. and Weeks, W. F.: Equations for determining the gas and brine volumes in sea-ice samples, J. Glaciol., 29(102), 306–316, 1983.

Crespo-Medina, M., Meile, C. D., Hunter, K. S., Diercks, A.-R., Asper, V. L., Orphan, V. J., Tavormina, P. L., Nigro, L. M., Battles, J. J., Chanton, J. P., Shiller, A. M., Joung, D.-J., Amon, R. M. W., Bracco, A., Montoya, J. P., Villareal, T. A.,

Wood, A. M. and Joye, S. B.: The rise and fall of methanotrophy following a deepwater oil-well blowout, Nat. Geosci., 7(6), 423–427, doi:10.1038/ngeo2156, 2014.

Damm, E., Mackensen, A., Budéus, G., Faber, E. and Hanfland, C.: Pathways of methane in seawater: Plume spreading in an Arctic shelf environment (SW-Spitsbergen), Cont. Shelf Res., 25(12–13), 1453–1472, doi:10.1016/j.csr.2005.03.003, 2005.

5 Damm, E., Kiene, R. P., Schwarz, J., Falck, E. and Dieckmann, G.: Methane cycling in Arctic shelf water and its relationship with phytoplankton biomass and DMSP, Mar. Chem., 109(1–2), 45–59, doi:10.1016/j.marchem.2007.12.003, 2008.

Damm, E., Helmke, E., Thoms, S., Schauer, U., Nöthig, E., Bakker, K. and Kiene, R. P.: Methane production in aerobic oligotrophic surface water in the central Arctic Ocean, Biogeosciences, 7(3), 1099–1108, doi:10.5194/bg-7-1099-2010, 2010.

10 Damm, E., Rudels, B., Schauer, U., Mau, S. and Dieckmann, G.: Methane exess in Arctic surface water - triggered by sea ice formation and melting, Sci. Rep., 2015.

Deutzmann, J. S., Worner, S. and Schink, B.: Activity and Diversity of Methanotrophic Bacteria at Methane Seeps in Eastern Lake Constance Sediments, Appl. Environ. Microbiol., 77(8), 2573–2581, doi:10.1128/AEM.02776-10, 2011.

Dunfield, P. F., Yuryev, A., Senin, P., Smirnova, A. V., Stott, M. B., Hou, S., Ly, B., Saw, J. H., Zhou, Z., Ren, Y., Wang, 15 J., Mountain, B. W., Crowe, M. A., Weatherby, T. M., Bodelier, P. L. E., Liesack, W., Feng, L., Wang, L. and Alam, M.: Methane oxidation by an extremely acidophilic bacterium of the phylum Verrucomicrobia, Nature, 450(7171), 879–882, doi:10.1038/nature06411, 2007.

Edgar, R. C., Haas, B. J., Clemente, J. C., Quince, C. and Knight, R.: UCHIME improves sensitivity and speed of chimera detection, Bioinformatics, 27(16), 2194–2200, doi:10.1093/bioinformatics/btr381, 2011.

20 Eronen-Rasimus, E., Luhtanen, A.-M., Rintala, J.-M., Delille, B., Dieckmann, G., Karkman, A. and Tison, J.-L.: An active bacterial community linked to high chl-a concentrations in Antarctic winter-pack ice and evidence for the development of an anaerobic sea-ice bacterial community, ISME J., doi:10.1038/ismej.2017.96, 2017.

Eyice, Ö., Namura, M., Chen, Y., Mead, A., Samavedam, S. and Schäfer, H.: SIP metagenomics identifies uncultivated Methylophilaceae as dimethylsulphide degrading bacteria in soil and lake sediment, ISME J., 9(11), 2336–2348, 25 doi:10.1038/ismej.2015.37, 2015.

Fish, J. A., Chai, B., Wang, Q., Sun, Y., Brown, C. T., Tiedje, J. M. and Cole, J. R.: FunGene: the functional gene pipeline and repository, Front. Microbiol., 4, doi:10.3389/fmicb.2013.00291, 2013.

Florez-Leiva, L., Tarifeño, E., Cornejo, M., Kiene, R. and Farías, L.: High production of nitrous oxide (N_2O), methane (CH_4) and dimethylsulphoniopropionate (DMSP) in a massive marine phytoplankton culture, Biogeosciences Discuss., 7(5), 6705–30 6723, doi:10.5194/bgd-7-6705-2010, 2010.

Formolo, M.: The microbial production of methane and other volatile hydrocarbons, in Handbook of Hydrocarbon and Lipid Microbiology, edited by K. N. Timmis, pp. 113–126, Springer Berlin Heidelberg, Berlin, Heidelberg. [online] Available from: http://link.springer.com/10.1007/978-3-540-77587-4_6 (Accessed 5 January 2017), 2010.

Gentz, T., Damm, E., Schneider von Deimling, J., Mau, S., McGinnis, D. F. and Schlüter, M.: A water column study of methane around gas flares located at the West Spitsbergen continental margin, Cont. Shelf Res., 72, 107–118, doi:10.1016/j.csr.2013.07.013, 2014.

Golden, K. M., Ackley, S. F. and Lytle, V. I.: The Percolation Phase Transition in Sea Ice, Science, 282(5397), 2238–2241, doi:10.1126/science.282.5397.2238, 1998.

Grant, N. J. and Whiticar, M. J.: Stable carbon isotopic evidence for methane oxidation in plumes above Hydrate Ridge, Cascadia Oregon Margin., Glob. Biogeochem. Cycles, 16(4), 71-1-71–13, doi:10.1029/2001GB001851, 2002.

Hakemian, A. S. and Rosenzweig, A. C.: The Biochemistry of Methane Oxidation, Annu. Rev. Biochem., 76(1), 223–241, doi:10.1146/annurev.biochem.76.061505.175355, 2007.

Hansman, R. L., Thurber, A. R., Levin, L. A. and Aluwihare, L. I.: Methane fates in the benthos and water column at cold seep sites along the continental margin of Central and North America, Deep Sea Res. Part Oceanogr. Res. Pap., 120, 122–131, doi:10.1016/j.dsr.2016.12.016, 2017.

Hanson, R. S. and Hanson, T. E.: Methanotrophic bacteria, Microbiol. Rev., 60(2), 439–471, 1996.

Heeschen, K. U., Keir, R. S., Rehder, G., Klatt, O. and Suess, E.: Methane dynamics in the Weddell Sea determined via stable isotope ratios and CFC-11, Glob. Biogeochem. Cycles, 18(2), n/a-n/a, doi:10.1029/2003GB002151, 2004.

Holmes, A. J., Roslev, P., McDonald, I. R., Iversen, N., Henriksen, K. and Murrell, J. C.: Characterization of Methanotrophic Bacterial Populations in Soils Showing Atmospheric Methane Uptake, Appl. Environ. Microbiol., 65(8), 3312–3318, 1999.

Hutchens, E., Radajewski, S., Dumont, M. G., McDonald, I. R. and Murrell, J. C.: Analysis of methanotrophic bacteria in Movile Cave by stable isotope probing: Methanotrophs in Movile Cave, Environ. Microbiol., 6(2), 111–120, doi:10.1046/j.1462-2920.2003.00543.x, 2003.

IPCC: Climate Change 2014: Mitigation of Climate Change. Contribution of Working Group III to the Fifth Assessment Report of the Intergovernmental Panel on Climate Change. Edenhofer, O., Pichs-Madruga, R., Sokona, Y., Farahani, E., Kadner, S., Seyboth, K., Adler, A., Baum, I., Brunner, S., Eickemeier, P., Kriemann, B., Savolainen, J., Schlömer, S., von Stechow, C., Zwickel, T., Minx J.C. (Eds). Cambridge University Press, Cambridge, United Kingdom and New York, NY, USA., 2014.

Jensen, S., Neufeld, J. D., Birkeland, N.-K., Hovland, M. and Murrell, J. C.: Methane assimilation and trophic interactions with marine Methylomicrobium in deep-water coral reef sediment off the coast of Norway: Deep-water coral reef methanotrophy, FEMS Microbiol. Ecol., 66(2), 320–330, doi:10.1111/j.1574-6941.2008.00575.x, 2008.

Karl, D. M., Beversdorf, L., Björkman, K. M., Church, M. J., Martinez, A. and Delong, E. F.: Aerobic production of methane in the sea, Nat. Geosci., 1(7), 473–478, 2008.

Katoh, K. and Standley, D. M.: MAFFT Multiple Sequence Alignment Software Version 7: Improvements in Performance and Usability, Mol. Biol. Evol., 30(4), 772–780, doi:10.1093/molbev/mst010, 2013.

Keir, R. S., Schmale, O., Seifert, R. and Sültenfuß, J.: Isotope fractionation and mixing in methane plumes from the Logatchev hydrothermal field, Geochem. Geophys. Geosystems, 10(5), n/a-n/a, doi:10.1029/2009GC002403, 2009.

Kessler, J. D., Valentine, D. L., Redmond, M. C., Du, M., Chan, E. W., Mendes, S. D., Quiroz, E. W., Villanueva, C. J., Shusta, S. S., Werra, L. M., Yvon-Lewis, S. A. and Weber, T. C.: A Persistent Oxygen Anomaly Reveals the Fate of Spilled Methane in the Deep Gulf of Mexico, Science, 331(6015), 312–315, doi:10.1126/science.1199697, 2011.

Kirst, G. O., Thiel, C., Wolff, H., Nothnagel, J., Wanzek, M. and Ulmke, R.: Dimethylsulfoniopropionate (DMSP) in ice-algae and its possible biological role, Mar. Chem., 35(1–4), 381–388, doi:10.1016/S0304-4203(09)90030-5, 1991.

Knief, C.: Diversity and Habitat Preferences of Cultivated and Uncultivated Aerobic Methanotrophic Bacteria Evaluated Based on pmoA as Molecular Marker, Front. Microbiol., 6, doi:10.3389/fmicb.2015.01346, 2015.

Knittel, K. and Boetius, A.: Anaerobic oxidation of methane: Progress with an unknown process, Annu. Rev. Microbiol., 63(1), 311–334, doi:10.1146/annurev.micro.61.080706.093130, 2009.

Krause, S. M. B., Johnson, T., Samadhi Karunaratne, Y., Fu, Y., Beck, D. A. C., Chistoserdova, L. and Lidstrom, M. E.: Lanthanide-dependent cross-feeding of methane-derived carbon is linked by microbial community interactions, Proc. Natl. Acad. Sci., 114(2), 358–363, doi:10.1073/pnas.1619871114, 2017.

Kvenvolden, K. A. and Rogers, B. W.: Gaia's breath—global methane exhalations, Mar. Pet. Geol., 22(4), 579–590, doi:10.1016/j.marpetgeo.2004.08.004, 2005.

Larkin, M. A., Blackshields, G., Brown, N. P., Chenna, R., McGettigan, P. A., McWilliam, H., Valentin, F., Wallace, I. M., Wilm, A., Lopez, R., Thompson, J. D., Gibson, T. J. and Higgins, D. G.: Clustal W and Clustal X version 2.0, Bioinformatics, 23(21), 2947–2948, doi:10.1093/bioinformatics/btm404, 2007.

Lecher, A. L., Kessler, J., Sparrow, K., Garcia-Tigreros Kodovska, F., Dimova, N., Murray, J., Tulaczyk, S. and Paytan, A.: Methane transport through submarine groundwater discharge to the North Pacific and Arctic Ocean at two Alaskan sites, Limnol. Oceanogr., 61(S1), S344–S355, doi:10.1002/lno.10118, 2016.

Leifer, I. and Patro, R. K.: The bubble mechanism for methane transport from the shallow sea bed to the surface: A review and sensitivity study, Cont. Shelf Res., 22(16), 2409–2428, doi:http://dx.doi.org/10.1016/S0278-4343(02)00065-1, 2002.

Loose, B., Schlosser, P., Perovich, D., Ringelberg, D., Ho, D. T., Takahashi, T., Richter-Menge, J., Reynolds, C. M., Mcgillis, W. R. and Tison, J.-L.: Gas diffusion through columnar laboratory sea ice: implications for mixed-layer ventilation of CO_2 in the seasonal ice zone., Tellus B, 63(1), 23–39, doi:10.1111/j.1600-0889.2010.00506.x, 2011.

Lorenson, T. D. and Kvenvolden, K. A.: Methane in coastal seawater, sea ice and bottom sediments, Beaufort Sea, Alaska: U.S. Geological Survey Open-File Report 95-70, US Geological Survey, Menlo Park, CA, 1995.

Lorenson, T. D., Greinert, J. and Coffin, R. B.: Dissolved methane in the Beaufort Sea and the Arctic Ocean, 1992-2009; sources and atmospheric flux: Dissolved methane in the Beaufort Sea and the Arctic Ocean, Limnol. Oceanogr., 61(S1), S300–S323, doi:10.1002/lno.10457, 2016.

Love, M. I., Huber, W. and Anders, S.: Moderated estimation of fold change and dispersion for RNA-seq data with DESeq2, Genome Biol., 15(12), doi:10.1186/s13059-014-0550-8, 2014.

Lüke, C. and Frenzel, P.: Potential of pmoA Amplicon Pyrosequencing for Methanotroph Diversity Studies, Appl. Environ. Microbiol., 77(17), 6305–6309, doi:10.1128/AEM.05355-11, 2011.

Lyew, D. and Guiot, S.: Effects of aeration and organic loading rates on degradation of trichloroethylene in a methanogenic-methanotrophic coupled reactor, Appl. Microbiol. Biotechnol., 61(3), 206–213, doi:10.1007/s00253-003-1224-8, 2003.

5   Magen, C., Lapham, L. L., Pohlman, J. W., Marshall, K., Bosman, S., Casso, M. and Chanton, J. P.: A simple headspace equilibration method for measuring dissolved methane, Limnol. Oceanogr. Methods, 12(9), 637–650, doi:10.4319/lom.2014.12.637, 2014.

Mau, S., Blees, J., Helmke, E., Niemann, H. and Damm, E.: Vertical distribution of methane oxidation and methanotrophic response to elevated methane concentrations in stratified waters of the Arctic fjord Storfjorden (Svalbard, Norway),
10   Biogeosciences, 10(10), 6267–6278, doi:10.5194/bg-10-6267-2013, 2013.

Mau, S., Römer, M., Torres, M. E., Bussmann, I., Pape, T., Damm, E., Geprägs, P., Wintersteller, P., Hsu, C.-W., Loher, M. and Bohrmann, G.: Widespread methane seepage along the continental margin off Svalbard - from Bjørnøya to Kongsfjorden, Sci. Rep., 7, 42997, doi:10.1038/srep42997, 2017.

McDonald, I. R., Bodrossy, L., Chen, Y. and Murrell, J. C.: Molecular Ecology Techniques for the Study of Aerobic
15   Methanotrophs, Appl. Environ. Microbiol., 74(5), 1305–1315, doi:10.1128/AEM.02233-07, 2008.

McKinney, C. R., McCrea, J. M., Epstein, S., Allen, H. A. and Urey, H. C.: Improvements in mass spectrometers for the measurement of small differences in isotope abundance ratios, Rev. Sci. Instrum., 21(8), 724, doi:10.1063/1.1745698, 1950.

McMurdie, P. J. and Holmes, S.: phyloseq: An R Package for Reproducible Interactive Analysis and Graphics of Microbiome Census Data, PLoS ONE, 8(4), e61217, doi:10.1371/journal.pone.0061217, 2013.

20   Murrell, J. C.: The aerobic methane oxidizing bacteria (Methanotrophs), in Handbook of Hydrocarbon and Lipid Microbiology, edited by K. N. Timmis, pp. 1953–1966, Springer Berlin Heidelberg, Berlin, Heidelberg. [online] Available from: http://link.springer.com/10.1007/978-3-540-77587-4_143 (Accessed 5 January 2017), 2010.

Nelson, M. C., Morrison, H. G., Benjamino, J., Grim, S. L. and Graf, J.: Analysis, Optimization and Verification of Illumina-Generated 16S rRNA Gene Amplicon Surveys, PLoS ONE, 9(4), e94249, doi:10.1371/journal.pone.0094249, 2014.

25   Oksanen, J., Blanchet, F. G., Friendly, M., Kindt, R., Legendre, P., McGlinn, D., Minchin, P. R., O'Hara, R. B., Simpson, G. L., Solymos, P., Stevens, M. H. H., Szoecs, E. and Wagner, H.: vegan: Community Ecology Package. [online] Available from: https://CRAN.R-project.org/package=vegan, 2017.

Oremland, R. S.: Methanogenic activity in plankton samples and fish intestines: A mechanism for in situ methanogenesis in oceanic surface waters, Limnol. Oceanogr., 24(6), 1136–1141, doi:10.4319/lo.1979.24.6.1136, 1979.

30   Overduin, P. P., Westermann, S., Yoshikawa, K., Haberlau, T., Romanovsky, V. and Wetterich, S.: Geoelectric observations of the degradation of nearshore submarine permafrost at Barrow (Alaskan Beaufort Sea), J. Geophys. Res. Earth Surf., 117(F2), n/a-n/a, doi:10.1029/2011JF002088, 2012.

Pol, A., Heijmans, K., Harhangi, H. R., Tedesco, D., Jetten, M. S. M. and Op den Camp, H. J. M.: Methanotrophy below pH 1 by a new Verrucomicrobia species, Nature, 450(7171), 874–878, doi:10.1038/nature06222, 2007.

Preuss, I., Knoblauch, C., Gebert, J. and Pfeiffer, E.-M.: Improved quantification of microbial CH_4 oxidation efficiency in arctic wetland soils using carbon isotope fractionation, Biogeosciences, 10(4), 2539–2552, doi:10.5194/bg-10-2539-2013, 2013.

Quast, C., Pruesse, E., Yilmaz, P., Gerken, J., Schweer, T., Yarza, P., Peplies, J. and Glockner, F. O.: The SILVA ribosomal RNA gene database project: improved data processing and web-based tools, Nucleic Acids Res., 41(D1), D590–D596, doi:10.1093/nar/gks1219, 2013.

R CoreTeam: R: A language and Environment for Statistical Computing. Available at: http://www.r-project.org/, 2015.

Rahalkar, M., Deutzmann, J., Schink, B. and Bussmann, I.: Abundance and Activity of Methanotrophic Bacteria in Littoral and Profundal Sediments of Lake Constance (Germany), Appl. Environ. Microbiol., 75(1), 119–126, doi:10.1128/AEM.01350-08, 2009.

Redmond, M. C., Valentine, D. L. and Sessions, A. L.: Identification of Novel Methane-, Ethane-, and Propane-Oxidizing Bacteria at Marine Hydrocarbon Seeps by Stable Isotope Probing, Appl. Environ. Microbiol., 76(19), 6412–6422, doi:10.1128/AEM.00271-10, 2010.

Reeburgh, W. S.: Methane consumption in Cariaco Trench waters and sediments, Earth Planet. Sci. Lett., 28(3), 337–344, doi:10.1016/0012-821X(76)90195-3, 1976.

Reeburgh, W. S.: Oceanic methane biogeochemistry, Chem. Rev., 107, 486–513, 2007.

Reeburgh, W. S., Ward, B. B., Whalen, S. C., Sandbeck, K. A., Kilpatrickt, K. A. and Kerkhof, L. J.: Black Sea methane geochemistry, Deep Sea Res. Part Oceanogr. Res. Pap., 38, S1189–S1210, doi:10.1016/S0198-0149(10)80030-5, 1991.

Repeta, D. J., Ferron, S., Sosa, O. A., Johnson, C. G., Repeta, L. D., Acker, M., DeLong, E. F. and Karl, D. M.: Marine methane paradox explained by bacterial degradation of dissolved organic matter, Nat. Geosci, 9(12), 884–887, 2016.

Rice, P., Longden, I. and Bleasby, A.: EMBOSS: The European Molecular Biology Open Software Suite, Trends Genet., 16(6), 276–277, doi:10.1016/S0168-9525(00)02024-2, 2000.

Roslev, P., Iversen, N. and Henriksen, K.: Oxidation and assimilation of atmospheric methane by soil methane oxidizers., Appl. Environ. Microbiol., 63(3), 874–880, 1997.

Saidi-Mehrabad, A., He, Z., Tamas, I., Sharp, C. E., Brady, A. L., Rochman, F. F., Bodrossy, L., Abell, G. C., Penner, T., Dong, X., Sensen, C. W. and Dunfield, P. F.: Methanotrophic bacteria in oilsands tailings ponds of northern Alberta, ISME J., 7(5), 908–921, doi:10.1038/ismej.2012.163, 2013.

Sansone, F. J., Popp, B. N., Gasc, A., Graham, A. W. and Rust, T. M.: Highly elevated methane in the eastern tropical North Pacific and associated isotopically enriched fluxes to the atmosphere, Geophys. Res. Lett., 28(24), 4567–4570, doi:10.1029/2001GL013460, 2001.

Saunois, M., Bousquet, P., Poulter, B., Peregon, A., Ciais, P., Canadell, J. G., Dlugokencky, E. J., Etiope, G., Bastviken, D., Houweling, S., Janssens-Maenhout, G., Tubiello, F. N., Castaldi, S., Jackson, R. B., Alexe, M., Arora, V. K., Beerling, D. J., Bergamaschi, P., Blake, D. R., Brailsford, G., Brovkin, V., Bruhwiler, L., Crevoisier, C., Crill, P., Covey, K., Curry, C., Frankenberg, C., Gedney, N., Höglund-Isaksson, L., Ishizawa, M., Ito, A., Joos, F., Kim, H.-S., Kleinen, T., Krummel, P.,

Lamarque, J.-F., Langenfelds, R., Locatelli, R., Machida, T., Maksyutov, S., McDonald, K. C., Marshall, J., Melton, J. R., Morino, I., Naik, V., O'Doherty, S., Parmentier, F.-J. W., Patra, P. K., Peng, C., Peng, S., Peters, G. P., Pison, I., Prigent, C., Prinn, R., Ramonet, M., Riley, W. J., Saito, M., Santini, M., Schroeder, R., Simpson, I. J., Spahni, R., Steele, P., Takizawa, A., Thornton, B. F., Tian, H., Tohjima, Y., Viovy, N., Voulgarakis, A., van Weele, M., van der Werf, G. R., Weiss, R., Wiedinmyer, C., Wilton, D. J., Wiltshire, A., Worthy, D., Wunch, D., Xu, X., Yoshida, Y., Zhang, B., Zhang, Z. and Zhu, Q.: The global methane budget 2000–2012, Earth Syst. Sci. Data, 8(2), 697–751, doi:10.5194/essd-8-697-2016, 2016.

Schloss, P. D., Westcott, S. L., Ryabin, T., Hall, J. R., Hartmann, M., Hollister, E. B., Lesniewski, R. A., Oakley, B. B., Parks, D. H., Robinson, C. J., Sahl, J. W., Stres, B., Thallinger, G. G., Van Horn, D. J. and Weber, C. F.: Introducing mothur: Open-Source, Platform-Independent, Community-Supported Software for Describing and Comparing Microbial Communities, Appl. Environ. Microbiol., 75(23), 7537–7541, doi:10.1128/AEM.01541-09, 2009.

Semrau, J. D., DiSpirito, A. A. and Yoon, S.: Methanotrophs and copper, FEMS Microbiol. Rev., 34(4), 496–531, doi:10.1111/j.1574-6976.2010.00212.x, 2010.

Shakhova, N., Semiletov, I., Salyuk, A., Yusupov, V., Kosmach, D. and Gustafsson, Ö.: Extensive methane venting to the atmosphere from sediments of the East Siberian Arctic shelf, Science, 327(5970), 1246–1250, doi:10.1126/science.1182221, 2010.

Steinle, L., Graves, C. A., Treude, T., Ferré, B., Biastoch, A., Bussmann, I., Berndt, C., Krastel, S., James, R. H., Behrens, E., Böning, C. W., Greinert, J., Sapart, C.-J., Scheinert, M., Sommer, S., Lehmann, M. F. and Niemann, H.: Water column methanotrophy controlled by a rapid oceanographic switch, Nat. Geosci., 8(5), 378–382, doi:10.1038/ngeo2420, 2015.

Steinle, L., Schmidt, M., Bryant, L., Haeckel, M., Linke, P., Sommer, S., Zopfi, J., Lehmann, M. F., Treude, T. and Niemannn, H.: Linked sediment and water-column methanotrophy at a man-made gas blowout in the North Sea: Implications for methane budgeting in seasonally stratified shallow seas: Linked sediment and water methanotrophy, Limnol. Oceanogr., 61(S1), S367–S386, doi:10.1002/lno.10388, 2016.

Stoddard, S. F., Smith, B. J., Hein, R., Roller, B. R. K. and Schmidt, T. M.: rrnDB: improved tools for interpreting rRNA gene abundance in bacteria and archaea and a new foundation for future development, Nucleic Acids Res., 43(D1), D593–D598, doi:10.1093/nar/gku1201, 2015.

Strong, P. J., Xie, S. and Clarke, W. P.: Methane as a Resource: Can the Methanotrophs Add Value?, Environ. Sci. Technol., 49(7), 4001–4018, doi:10.1021/es504242n, 2015.

Tanaka, K., Takesue, N., Nishioka, J., Kondo, Y., Ooki, A., Kuma, K., Hirawake, T. and Yamashita, Y.: The conservative behavior of dissolved organic carbon in surface waters of the southern Chukchi Sea, Arctic Ocean, during early summer, Sci. Rep., 6(1), doi:10.1038/srep34123, 2016.

Tavormina, P. L., Ussler, W. and Orphan, V. J.: Planktonic and Sediment-Associated Aerobic Methanotrophs in Two Seep Systems along the North American Margin, Appl. Environ. Microbiol., 74(13), 3985–3995, doi:10.1128/AEM.00069-08, 2008.

Thomas, D. N. and Dieckmann, G. S.: Antarctic Sea Ice–a Habitat for Extremophiles, Science, 295(5555), 641–644, doi:10.1126/science.1063391, 2002.

Tsunogai, U., Yoshida, N., Ishibashi, J. and Gamo, T.: Carbon isotopic distribution of methane in deep-sea hydrothermal plume, Myojin Knoll Caldera, Izu-Bonin arc: implications for microbial methane oxidation in the oceans and applications to heat flux estimation, Geochim. Cosmochim. Acta, 64(14), 2439–2452, doi:10.1016/S0016-7037(00)00374-4, 2000.

Uhlig, C. and Loose, B.: Using stable isotopes and gas concentrations for independent constraints on microbial methane oxidation at Arctic Ocean temperatures: Methane oxidation rates from stable isotopes, Limnol. Oceanogr. Methods, doi:10.1002/lom3.10199, 2017.

Valentine, D. L., Blanton, D. C., Reeburgh, W. S. and Kastner, M.: Water column methane oxidation adjacent to an area of active hydrate dissociation, Eel river Basin, Geochim. Cosmochim. Acta, 65(16), 2633–2640, doi:10.1016/S0016-7037(01)00625-1, 2001.

Valentine, D. L., Kessler, J. D., Redmond, M. C., Mendes, S. D., Heintz, M. B., Farwell, C., Hu, L., Kinnaman, F. S., Yvon-Lewis, S., Du, M., Chan, E. W., Tigreros, F. G. and Villanueva, C. J.: Propane respiration jump-starts microbial response to a deep oil spill, Science, 330(6001), 208–211, doi:10.1126/science.1196830, 2010.

Verdugo, J., Damm, E., Snoeijs, P., Díez, B. and Farías, L.: Climate relevant trace gases (N_2O and CH_4) in the Eurasian Basin (Arctic Ocean), Deep Sea Res. Part Oceanogr. Res. Pap., 117, 84–94, doi:10.1016/j.dsr.2016.08.016, 2016.

Vrede, K., Heldal, M., Norland, S. and Bratbak, G.: Elemental Composition (C, N, P) and Cell Volume of Exponentially Growing and Nutrient-Limited Bacterioplankton, Appl. Environ. Microbiol., 68(6), 2965–2971, doi:10.1128/AEM.68.6.2965-2971.2002, 2002.

Wang, S. W., Budge, S. M., Gradinger, R. R., Iken, K. and Wooller, M. J.: Fatty acid and stable isotope characteristics of sea ice and pelagic particulate organic matter in the Bering Sea: tools for estimating sea ice algal contribution to Arctic food web production, Oecologia, 174(3), 699–712, doi:10.1007/s00442-013-2832-3, 2014.

Whiticar, M. J.: Carbon and hydrogen isotope systematics of bacterial formation and oxidation of methane, Chem. Geol., 161(1–3), 291–314, doi:10.1016/S0009-2541(99)00092-3, 1999.

Yamamoto, S., Alcauskas, J. B. and Crozier, T. E.: Solubility of methane in distilled water and seawater, J. Chem. Eng. Data, 21(1), 78–80, doi:10.1021/je60068a029, 1976.

Zhivotchenko, A. G., Nikonova, E. S. and Jørgensen, M. H.: Copper effect on the growth kinetics of *Methylococcus capsulatus (bath)*, Biotechnol. Tech., 9(3), 163–168, doi:10.1007/BF00157072, 1995.

Zhou, J., Tison, J.-L., Carnat, G., Geilfus, N.-X. and Delille, B.: Physical controls on the storage of methane in landfast sea ice, The Cryosphere, 8(3), 1019–1029, doi:10.5194/tc-8-1019-2014, 2014.
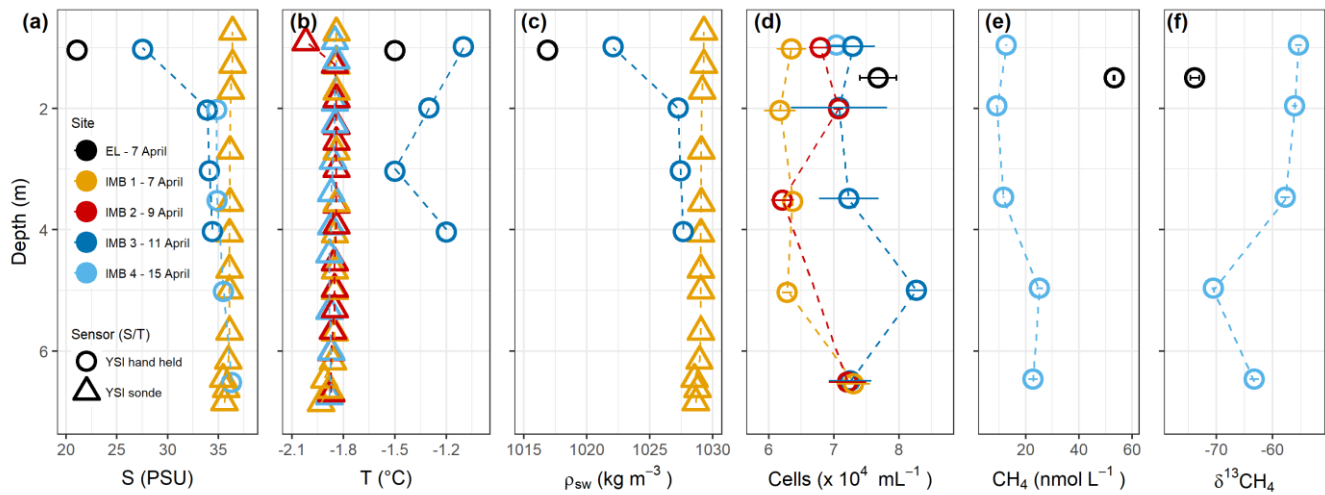
Figure 1: Water column properties during the time series near Utqiagvik. Salinity (a), temperature (b), density (c), cell abundance (d), methane concentration (a) and stable isotope ratios (b). Error bars on cell numbers (d) represent the standard deviation on two technical replicates. Temperature and salinity were determined with an YSI hand held (circle) and YSI sonde (triangle). Salinity for the YSI hand held on 15 April was determined with in the laboratory, thus in situ temperature is missing. Salinity for the YSI sonde on 9 and 15 April is missing due to freezing of the sensor. Methane data is only available for EL at 7 April and for IMB 4 at 15 April.
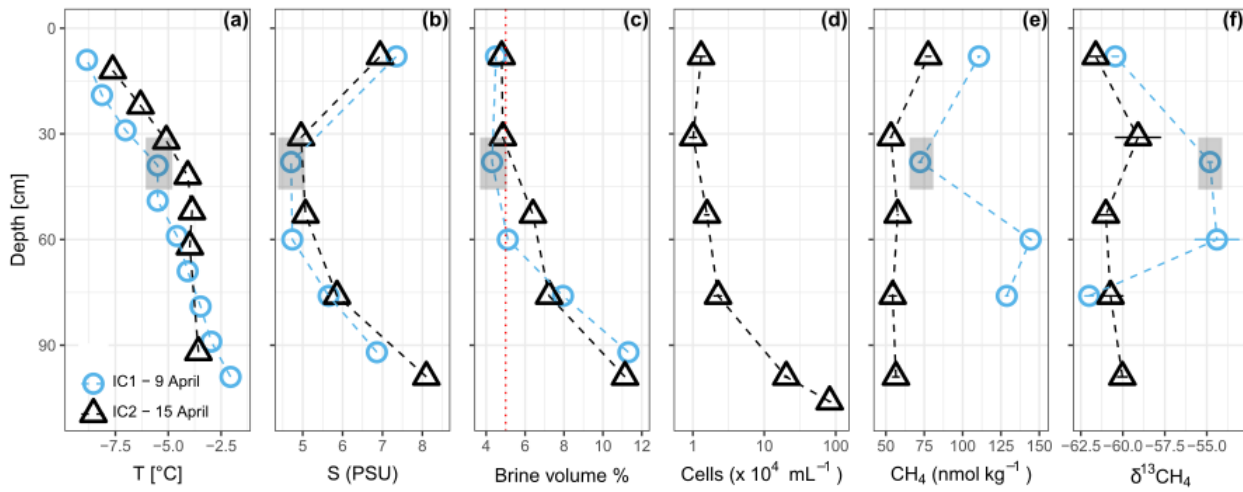
Figure 2: Sea ice temperature (a), bulk salinity (b), brine volume fraction (c), prokaryotic cells mL^{-1} sea ice (for IC2 only) (d), methane concentration (e) and stable isotope ratios (f). The vertical red dotted line in (c) shows a brine volume fraction of 5%, the threshold for permeability (Golden et al., 1998). IC1 had sediment included into the ice matrix at depth 30–46 cm, indicated by the gray box.
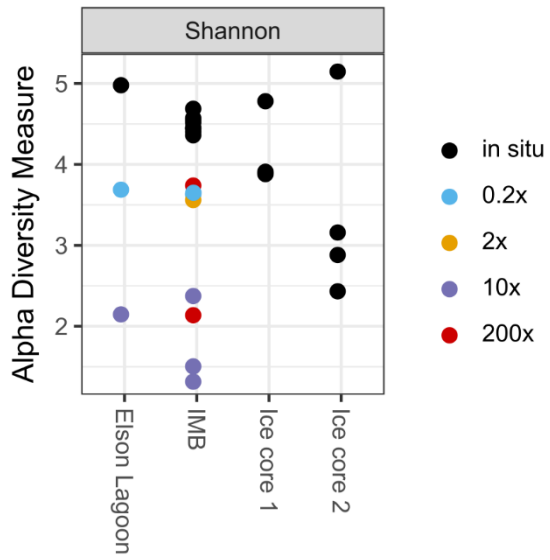
Figure 3: Shannon indices of alpha diversity for V4-V5 amplicons.
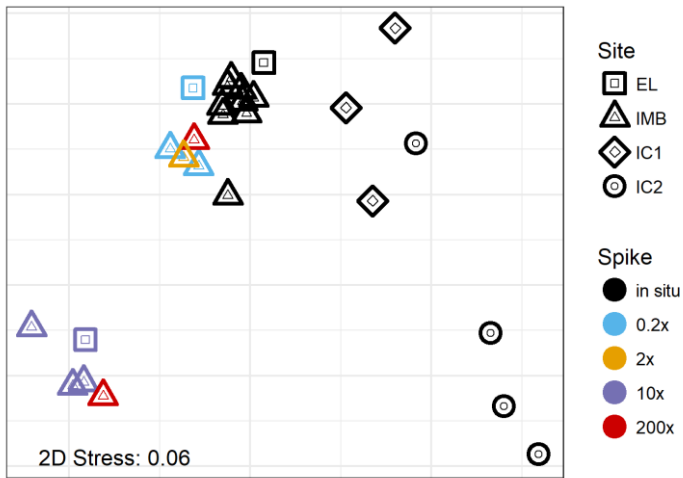
Figure 4: Non-metric multidimensional scaling analysis (unitless) of Bray-Curtis dissimilarities of the 16S read data. The low 2D stress of 0.06 indicates a good two-dimensional representation of the multidimensional dataset with very low prospect of misinterpretation.
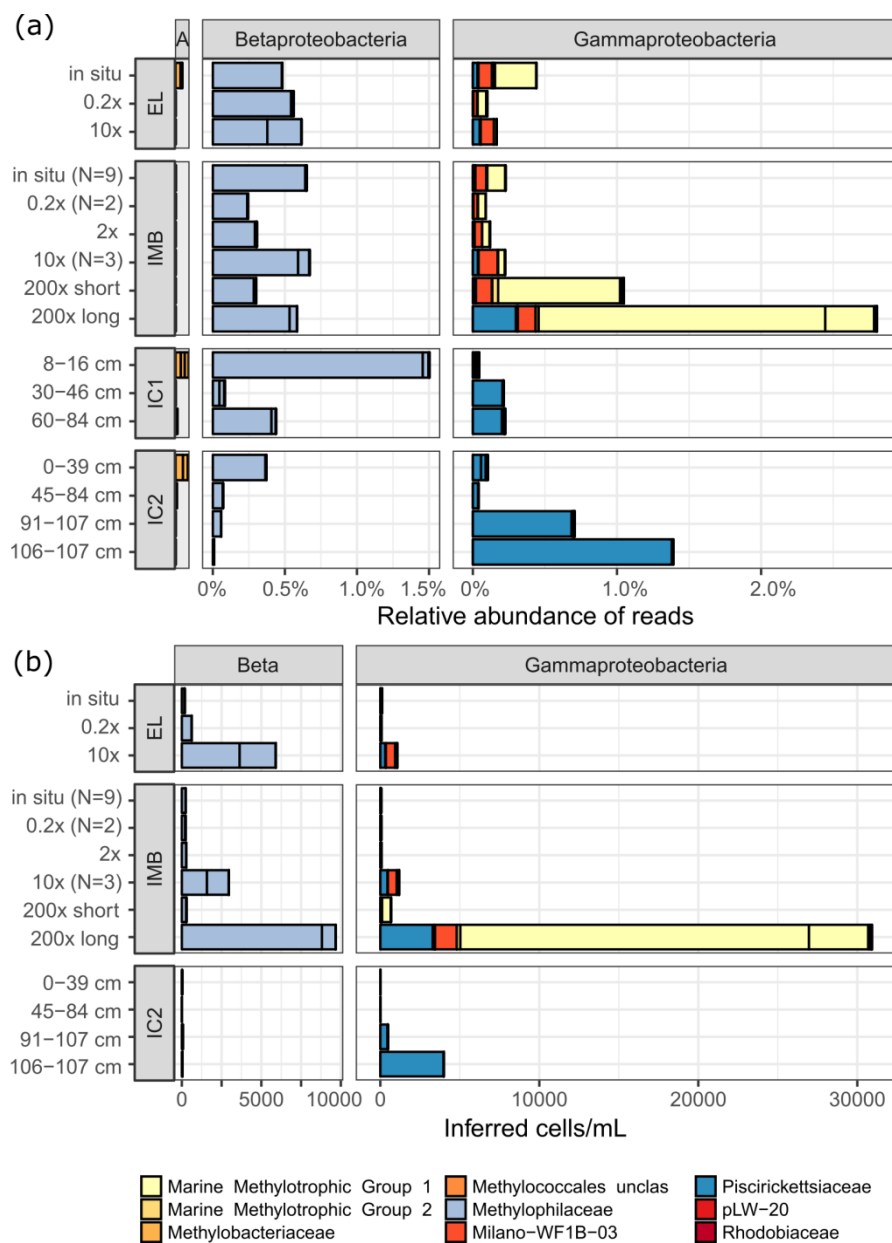
Figure 5: Relative abundances (a) and inferred cell numbers (b) of methylotroph OTUs by family. Sampling sites for water samples are Elson Lagoon (EL) and mass balance buoy (IMB). Ice cores (IC1 and IC2) were collected at site IMB on 9 and 15 April, respectively. The sample name indicates the methane spike concentration compared to in situ methane concentration for IMB and EL, and the ice core section in cm from top (0 cm, ice-snow interface) to bottom (ice-water interface). IMB in situ, 0.2x and 10x are averages of the respective number (N) of samples, all other samples were N=1. Red and yellow shades indicate MOB, while blue shades indicate non-MOB-methylotrophs. (a) α-Proteobacteria (A), β-Proteobacteria (Beta) and γ-Proteobacteria are shown; Verrucomicrobia Incertae Sedis were < 0.003% in (a). Scale for α-Proteobacteria is the same as for β- and γ-

Proteobacteria. (b) Cell numbers were calculated from the relative abundances shown in (a) with the cell counts from flow cytometry and corrected for the 16S copy number per cell. Verrucomicrobia Incertae Sedis and α-Proteobacteria were < 8 cells mL^{-1}.
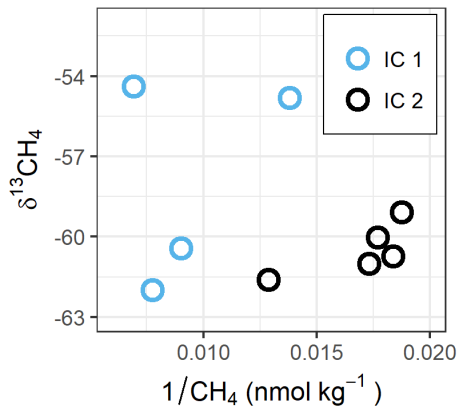
Figure 6: δ¹³CH₄ vs. reciprocal of CH₄ concentration (Keeling type plot) of ice cores. Within each ice core a shift to more positive δ¹³CH₄ values in combination with a decrease in CH₄ concentration indicates microbial oxidation. Comparing IC2 to IC1, the shift toward higher concentrations and more positive δ¹³CH₄ (see also Fig. 2) in IC1 might indicate CH₄ production from a substrate with heavier isotope signature, compared to the values in IC2.
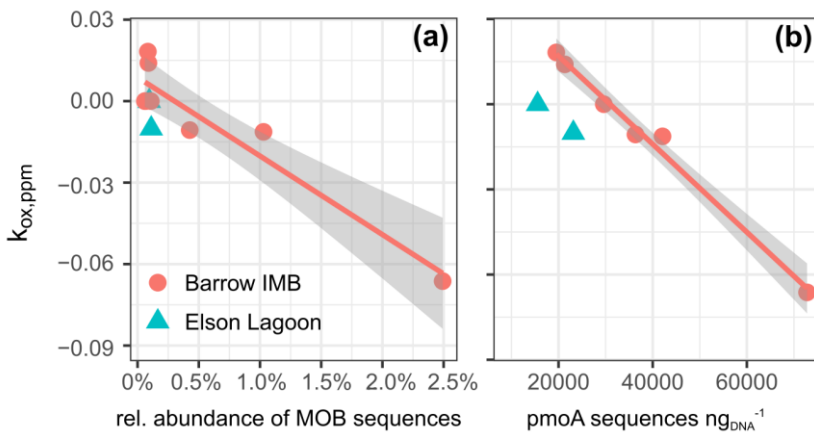
Figure 7: Correlation between net oxidation rate constant ($k_{ox,ppm}$) and the relative abundance of sequences in 16S-´MOB´-OTUs, $R^2_{(MOB-OUTs~kox)} = 0.84$ (a) and number of pmoA sequences with $R^2_{(pmoA~kox)} = 0.85$ (b). For correlation to the number of total methylotroph OTUs (which includes MOB and non-MOB-methylotrophs in total 16S) $R^2_{(´Meth´-OUTs~kox)} = 0.81$. The gray shaded area shows the 95% confidence interval of the correlation.
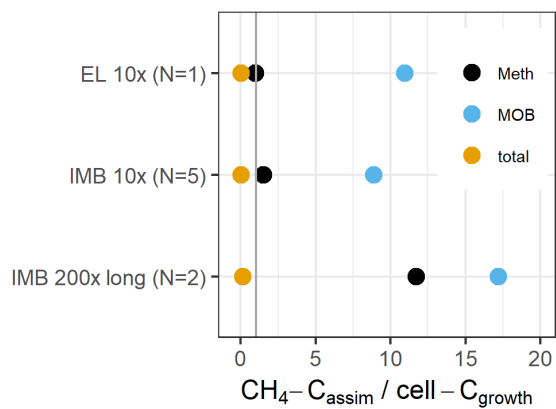
Figure 8: Ratio of methane-carbon assimilated (CH₄-C_assim) to cell-C gained during growth (cell-C_growth), based on flow cytometric cell counts (total) or inferred cell numbers (Meth, MOB). The standard deviation between replicates was 10–20%. The vertical line indicates a ratio of 1. Above 1, the entire cell gain can be explained by the assimilated CH₄.

Table 1: Station and sample list

Name[1]	Date	Position	Samples	Parameters[2]
EL	07.04.2016	71.334° N, -156.363° W	water	in situ CH_4, ox rate, T/S, DNA, cell counts, nutrients
IMB 1	07.04.2016	71.373° N, -156.548° W	water	ox rate, DNA[3], cell counts, nutrients[3]
IMB 2	09.04.2017	71.372° N, -156.540° W	water	ox rate, T, DNA[3], cell counts, nutrients[3]
			ice core 1	in situ CH_4, T/S, DNA
IMB 3	11.04.2015	71.372° N, -156.540° W	water	T/S[3], DNA, nutrients, cell counts
IMB 4	15.04.2017	71.372° N, -156.540° W	water	in situ CH_4, T/S, DNA[3]
			ice core 2	in situ CH_4, T/S, DNA, cell counts

[1]Station abbreviations are Elson Lagoon (EL) and ice mass balance buoy (IMB)

[2]Parameters: in situ concentration and $\delta^{13}CH_4$ (in situ CH_4), net oxidation/production rate (ox rate), temperature and salinity (T/S), collection of biomass for DNA extraction (DNA), cell counts, nutrients

5   [3]No complete depth profile available

Table 2: Samples sequenced for V4-V5 and pmoA

Treatment[1]	Station	V4-V5 # of samples	pmoA # of samples
in situ	IMB	9	4
	EL	1	1
	sea ice	7	0
0.2x, 10 days	IMB 1	2	3
	EL	1	1
2x, 5 days	IMB 2	1	1
10x, 46 days	IMB 1	3	2
	EL	1	1
200x, 6 days	IMB 2	1	1
200x, 41 days	IMB 2	1	1

[1]The different incubation times resulted from logistical constraints

Table 3: Methane oxidation parameters during long-term incubation experiments. N: number of replicates, $c(CH_4)_{initial}$: approximate initial methane concentration, $k_{ox,ppm}$: net oxidation/production rate constant, $r_{ox,ppm}$: net oxidation/production rate at in situ concentration, α_{ox}: isotopic fractionation factor during oxidation. Oxidation rates and rate constants are replicated from Uhlig and Loose (2017).

Treatment	N[1]	Incubation[2] [days]	$c(CH_4)_{initial}$ [nmol L^{-1}]	$c(CH_4)_{final}$ [nmol L^{-1}]	$k_{ox,ppm}$ [d^{-1}]	$r_{ox,ppm}$ [nmol L^{-1} d^{-1}]	α_{ox}
0.2x EL	1	10	12.7	12.9	0[3]	0[1]	0.9591
10x EL	1	46	132.3	67.7	1.01×10^{-2}	0.54	1.0230
0.2x IMB 1	5	10	4.4 ± 0.5	5.0 ± 0.4	-1.05×10^{-2}	Negative[4]	0.994 ± 0.0113
2x IMB 2	4	5	37.9 ± 1.8	36.5 ± 1.4	0[3]	0[3]	0.9898 ± 0.0104
10x IMB 1	5	46	123.0 ± 5.5	69.4 ± 36.5	9.18×10^{-3}	0.15 ± 0.02	1.0225 ± 0.0005
200x IMB 2 short	7	6	3937.9 ± 148.7	3427.6 ± 160.4	0[3]	0[3]	1.0005 ± 0.0005
200x IMB 2 long	2	41	4089.5 ± 26.1	129.6 ± 95.5	6.62×10^{-2}	1.08 ± 0.17	1.0103 ± 0.0002
200x IMB 2 NaOH	1	41	3953.7	3620.7	0[3]	0[3]	0.9998

[1]Replicates are from different water depth

[2]The different incubation times resulted from logistical constraints

[3]Oxidation rate constants were not significantly different from 0 at a 95% confidence level

[4]Negative net oxidation rate constant indicating methane production

Table 4: Relative abundance of Methylotroph-OTUs in situ, split into methanotrophs (MOB) and non-MOB-methylotrophs ("Methy")

		in situ sea ice	in situ sea water	0.2x, 2x (short)	10x (long)	200x (long+short)
N		7	10	4	4	2
Mean ± sd	MOB	0.04% ± 0.04%	0.24% ± 0.09%	0.09% ± 0.01%	0.17% ± 0.15%	1.76% ± 0.73%
	Methy	0.74% ± 0.50%	0.65% ± 0.12%	0.34% ± 0.13%	0.70% ± 0.62%	0.61% ± 0.29%
min	MOB	0.00%	0.06%	0.08%	0.06%	1.03%
	Methy	0.11%	0.51%	0.23%	0.20%	0.32%
max	MOB	0.11%	0.45%	0.11%	0.43%	2.49%
	Methy	1.53%	0.83%	0.56%	1.72%	0.90%

Table 5: Spearman rank order correlations coefficients (ρ_S) of $k_{ox,ppm}$ vs. the number of sequences of pmoA MOB and non-MOB methylotrophs, and candidate OTUs

	Total	Normalized[2]	Relative abundance	Inferred cell density[3]
pmoA	-0.86**[3]	n.d.	n.d.	n.d.
methylotrophs	-0.81**	-0.97***	-0.79**	-0.63.
MOB	-0.82**	-0.66*	-0.82**	-0.61.
non-MOB	-0.71*	-0.80**	-0.69*	-0.58.
candidate OTUs[4]	-0.07 ns	-0.23 ns	-0.03ns	n.d.

[1]Levels: $\rho_S < 0.8$ very strong, $0.6 < \rho_S < 0.8$ strong

[2]normalized to total abundance of reads using the DESeq2 package

5   [3]MOB cell density was calculated from relative abundance and flow cytometry cell counts, weighted for copy number of 16S for respective OTUs

[4]Significance levels: 0 '***' 0.001 '**' 0.01 '*' 0.05 '.' 0.1 'ns ' 1

[5]Candidate OTUs are OTUs that were differentially more abundant in 10x and 200x incubated samples